UNIVERSITÉ DU QUÉBEC À MONTRÉAL

CONTRÔLES BIOGÉOCHIMIQUES DES CONCENTRATIONS ET EXPORTS DE MERCURE (HG) DANS LES GRANDES RIVIÈRES NORDIQUES

MÉMOIRE

PRÉSENTÉ(E)

COMME EXIGENCE PARTIELLE

MAÎTRISE EN BIOLOGIE

PAR

CAROLINE FINK-MERCIER

AOÛT 2021

REMERCIEMENTS

Je tiens à remercier mes co-superviseurs Paul del Giorgio et Jean-François Lapierre pour cette opportunité de projet unique, aux paysages bouleversants, ainsi que pour leur soutien tout au long de ma maîtrise. Merci également aux nombreux membres du laboratoire del Giorgio qui ont activement participé aux campagnes d'échantillonnages soit Serge Paquet, Marie-Laure Gérardin, Alexandre Ducharme, Étienne Gauthier-Dufour, Joan Pere Casas Ruiz, Charles Charrier Tremblay, Éric Guimond, Alice Parkes, et plus spécialement à Karelle Desrosiers et Jean-Christophe Sicotte-Brisson pour leurs oreilles et leur folie qui ont grandement contribué aux gais souvenirs que je retire de cette expérience. En laboratoire, merci à Dominic Bélanger de m'avoir guidé dans les analyses et pour son sourire contagieux. Un gros merci à l'équipe du Conseil de l'Eau Gaspésie Sud pour l'opportunité de stage mémorable. Finalement, un merci spécial à mon copain Étienne et ses talents de cuisinier qui ont su nourrir mon corps et mon esprit tout au long de mon cheminement.

AVANT-PROPOS

Ce mémoire est séparé en quatre sections comprenant une introduction, deux chapitres sous forme d'articles scientifiques et une conclusion générale. L'introduction fait un survol des connaissances actuelles et de ses lacunes, puis énonce les objectifs et les hypothèses. Le premier chapitre du mémoire porte sur les éléments du paysage influençant les concentrations ainsi que les exports de mercure (Hg) et méthylmercure (MeHg) dans les grandes rivières nordiques de la Baie James. Le second chapitre adresse les facteurs influençant la variation du couplage du Hg et du MeHg avec le carbone organique dissout (COD) dans ces mêmes grandes rivières nordiques. Les deux articles ont été rédigés en anglais afin de publier dans des journaux scientifiques anglophones éminemment. La conclusion présente un résumé des connaissances apportées à la communauté scientifique grâce aux études réalisées dans le cadre de ce mémoire.

TABLE DES MATIÈRES

LISTE DES FIGURES

LISTE DES TABLEAUX

LISTE DES ABRÉVIATIONS, DES SIGLES ET DES ACRONYMES

CDOM :	Coloured dissolved organic matter
COD / DOC :	Carbone organique dissout / Dissolved organic carbon
CVAFS :	Cold vapour atomic fluorescence spectroscopy
δ18O :	Ratio d'oxygène 18
δ2H :	Ratio d'hydrogène 2
d-excess :	Deuterium excess
FDOM :	Fluorescent dissolved organic matter
HDPE :	High-density polyethylene
Hg :	Mercure / Mercury
Hg(0) :	Mercure élémentaire
Hg(II) :	Mercure ionique
MeHg :	Méthylmercure / Methylmercury
VSMOW2 :	Vienna Standard Mean Ocean Water 2
SLAP :	Standard light Antarctic precipitation

SUVA : Specific ultraviolet absorbance

UV254 : UV absorbance at 254 nm

R^2 : Coefficient of corrélation

RÉSUMÉ

Les grandes rivières nordiques sont un vecteur majeur de Hg vers l'océan Arctique. Toutefois, à grande échelle, les mécanismes d'apport, de perte et de transformation de ce Hg le long du continuum de rivière restent méconnus. Dans cette étude, nous identifions les sources et les puits de Hg au cours d'un cycle annuel dans 18 grandes rivières de la Baie James (Québec) dont les bassins versants totalisent plus de 350 000 km^2, couvrant un impressionnant gradient en terme de couverture du sol, de température et d'hydrologie. Nos résultats démontrent que les plans d'eau dans le bassin versant influencent drastiquement les concentrations et exports de Hg et MeHg, suggérant qu'à grande échelle, les lacs sont des puits importants régulant les exports de Hg vers l'océan. Nous explorons ensuite le couplage du Hg avec le COD , un élément clé facilitant les apports de Hg terrestre vers les systèmes aquatiques. Nous démontrons que, bien que le COD explique une partie importante des patrons spatiotemporels de Hg et MeHg, les relations Hg-COD et MeHg-COD sont hautement variables et dépendent de la saisonnalité et de l'hydrologie du système. Ces résultats remettent en question l'utilisation du COD comme indicateur des concentrations et exports de Hg et soulignent l'influence de l'hydrologie sur les patrons de Hg, MeHg et COD dans les grandes rivières nordiques.

Mots clés : Mercure, méthylmercure, grandes rivières, boréal, couverture du paysage, carbone organique dissout, hydrologie, saisonnalité, exports

ABSTRACT

Large rivers are major contributors of Hg to the Arctic Ocean. Nevertheless, at broad scale, knowledge on loading, sink and transformation mechanisms of Hg along the aquatic network is still limited. In this study, we identify seasonal sources and sinks of Hg in 18 large rivers of James Bay (Québec) collectively draining over 350 000 km^2 and covering an important gradient in terms of landcover, temperature and hydrology. Our results show that water surface coverage in the watershed is the major landscape driver of both Hg and MeHg concentrations and exports. This suggests that at the whole network scale, this aquatic sink is the major regulating factor of Hg export to the ocean. We then explore the coupling between Hg and DOC, a key driver of Hg loading from terrestrial to aquatic systems. We demonstrate that although DOC explains a large portion of the variation in Hg and MeHg concentrations, Hg-DOC and MeHg-DOC relationships are highly variable and depend on seasonality and hydrology of the system. Our results challenge the use of DOC as an indicator of Hg concentrations and exports and highlight the role of hydrology in governing Hg, MeHg and DOC patterns in northern rivers.

Keywords : Mercury, methylmercury, large rivers, boreal, landcover, dissolved organic carbon, hydrology, seasonality, exports

INTRODUCTION

Le mercure est un élément naturel présent dans tous les écosystèmes (AMAP/UNEP, 2013). Cependant, les augmentations des émissions atmosphériques dans le dernier siècle ont fait augmenter les concentrations au-delà des niveaux naturels, faisant du Hg un contaminant environnemental répandu à l'échelle globale. (UN Environment, 2019). Sa répartition dans les écosystèmes est préoccupante notamment en raison de ses impacts sur la santé neurologique humaine (Cariccio et al., 2019). En particulier, la forme méthylée du mercure, le méthylmercure (MeHg), est bioaccumulable et bioamplifiable à travers le réseau alimentaire aquatique (Lescord et al., 2019), exposant les populations à forte diète piscivore à un risque accru d'intoxication chronique (Mason et al., 2012). L'incident de Minamata dans les années 1950 et 1960 a d'ailleurs été un exemple marquant d'exposition humaine au Hg via l'alimentation alors que des milliers de citoyens ont consommé des ressources halieutiques contaminées et soufferts des effets délétères du Hg (Takizawa, 1979). Cet événement a grandement contribué à conscientiser les acteurs globaux à sa toxicité et a éventuellement mené à la signature de la convention de Minamata, ciblant des efforts de réduction des émissions dans 128 pays (UN Environment, 2021).

Bien qu'une réduction des concentrations atmosphériques a été consignée depuis 1990 (Obrist et al., 2018), les écosystèmes nordiques continuent d'enregistrer des concentrations en Hg élevées dans la faune aquatique (Hare et al., 2008; Lockhart

et al., 2005). Ce Hg provient notamment du transport sur de longues distances des émissions d'origine humaine qui restent considérables (UN Environment, 2019). On estime ainsi que la déposition des émissions anthropiques a globalement doublé le réservoir de Hg emmagasiné dans les sols (Amos et al., 2013; Obrist et al., 2018). Par ailleurs, de récentes études projettent que ce Hg historiquement emmagasiné dans les sols nordiques sera relargué vers les écosystèmes aquatiques avec les changements climatiques lors de la fonte du pergélisol (Schuster et al., 2018). L'intensification projetée des régimes hydrologiques, traduites par des pluies plus fortes et abondantes ainsi que des cours d'eau aux débits plus intenses, augmentera également le lessivage du Hg terrestre (Guay et al., 2015; St. Pierre et al., 2018; Zolkos et al., 2020). Il est donc d'autant plus important de s'attarder au problème de Hg dans l'environnement nordique en raison des changements climatiques qui risquent de neutraliser les récents efforts de réduction des flux via la remise en circulation de Hg terrestre, auparavant séquestré, vers les lacs, rivières et océans.

Les grandes rivières nordiques, qui s'étendent de l'écosystème boréal à l'environnement arctique, jouent un rôle important dans le transport de ce nouveau et ancien Hg des systèmes terrestres vers l'océan Arctique (Fisher et al., 2012). Bien qu'elles soient loin des points sources d'émissions, elles exportent annuellement 37 000 kg de Hg (Zolkos et al., 2020), contribuant à 25% des apports externes en Hg dans l'océan Arctique alors que les rivières représentent environ 1% de ses afflux hydrologiques (Soerensen et al., 2016, Supporting informations). Le transport de ce

mercure par les rivières pose problème puisqu'il sédimente majoritairement sur les côtes des océans (Sunderland & Mason, 2007), affectant les organismes côtiers et exposant les populations autochtones nordiques au Hg via leur diète qui dépend grandement de la faune aquatique (Braune et al., 2005; Stow et al., 2011). L'identification des rivières à risque de transporter davantage de Hg pourrait permettre de connaître les régions susceptibles d'être exposées à de hautes concentrations en Hg. Cependant, l'identification de ces rivières à l'aide des modèles de transport globaux est ardue puisque des zones géographiquement rapprochées peuvent avoir des concentrations et des exports très variables indépendamment de la déposition atmosphérique (Domagalski et al., 2016; Eklof et al., 2012). De nombreuses études se sont donc concentrées sur les mécanismes d'apports et de perte de Hg dans les systèmes aquatiques à l'échelle locale dans le but de comprendre les patrons hétérogènes de Hg dans les rivières (Burns et al., 2013; Schelker et al., 2011; Vermilyea et al., 2017; Vidon et al., 2014). L'acquisition de connaissances sur les sources et les puits de Hg pourrait ainsi nous permettre de raffiner les bilans à grande échelle et de prédire les variations futures dans les exports riverains.

0.1 Sources et puits de Hg dans les bassins versants nordiques

Les sources de Hg dans les écosystèmes aquatiques peuvent être naturelles, telles que les feux de forêt, l'érosion de matériel géologique ou les volcans (Wang et al.,

2004), mais proviennent majoritairement de la déposition atmosphérique d'émission urbaine ou industrielle, principalement par la combustion d'énergies fossiles et l'extration minière artisanale (UN Environment, 2019) (UNEP 2018) (Figure 0.1). Lorsqu'il est oxydé, le Hg se dépose surtout sur les sols et la végétation (Graydon et al., 2008; Lindqvist et al., 1991). En effet, puisque la canopée augmente la surface de déposition du mercure atmosphérique, la déposition via l'interception par la végétation contribue de 54 à 94% du Hg dans les sols (Obrist et al., 2018). Le Hg est ensuite surtout co-mobilisé vers les écosystèmes aquatiques avec le carbone organique dissout (COD) en raison de l'affinité du Hg pour les groupements riches en thiols de la matière organique qui facilitent la complexation du Hg avec le COD et qui favorise subséquemment leur co-transport (Mierle & Ingram, 1991; Ravichandran, 2004; Riscassi & Scanlon, 2011). Grigal et al. (2002) soutient d'ailleurs qu'un ratio de 0.2 ng Hg par mg COD est généralement observé dans les lacs et rivières de l'hémisphère nord, soulignant un couplage COD-Hg répandu à travers les écosystèmes. Le Hg est ainsi majoritairement transporté avec le COD des sols vers les écosystèmes aquatiques durant les événements hydrologiques.

Une fois présent dans les lacs et rivières, le Hg peut être transformé et perdu. Dans des conditions de température, d'oxygène, de nutriments et de pH adéquats, ainsi qu'avec la présence de matière organique, le Hg peut être transformé en MeHg par les bactéries et archées encodant les gènes *hgcAB* (Gilmour et al., 2013; Tjerngren et al., 2012; Ullrich et al., 2001). Précisément, la matière organique d'origine microbienne a

récemment été identifiée comme contrôlant la production de MeHg (Bravo et al., 2018). Le Hg peut également être photodégradé, représentant un mécanisme majeur de perte où le Hg(II) est réduit en Hg(0), sa forme volatile, et où le MeHg est transformé en Hg(II) (Sellers et al., 2001). La sédimentation est également un puits de Hg, particulièrement dans les zones de faible courant (Selvendiran et al., 2009). Les formes aquatiques de Hg peuvent aussi être retirées via la consommation directe dans l'eau par les organismes. Cette voie est cependant mineure alors que la majorité du Hg et MeHg retrouvée dans les poissons proviennent de leur diète (Hall et al., 1997). Une fois apportés dans le continuum aquatique, le Hg et le MeHg peuvent donc être graduellement perdus ou transformés le long de leur transit vers l'embouchure.

Ces apports et ces pertes de Hg sont, en outre, influencés par des variables environnementales qui changent avec les saisons. Les forts débits printaniers associés à la fonte des neiges peuvent représenter près de la moitié des apports annuels en Hg vers les écosystèmes aquatiques (Zolkos et al., 2020). En contrepartie, ces conditions sont peu propices à la formation de MeHg et aux pertes par photodégradation et sédimentation (Schelker et al., 2011; Sellers et al., 2001; Selvendiran et al., 2009; Shanley et al., 2005). À l'opposé, les hautes températures, liées à des taux métaboliques élevés, ainsi que l'anoxie et les temps de rétention plus longs durant l'été sont liés à une grande production de MeHg (Babiarz et al., 1998; Selvendiran et al., 2008b). Les faibles débits estivaux sont également liés à de plus faibles apports en Hg (Schelker et al., 2011) et à de plus grandes pertes par photodégradation (Sellers et al., 2001). Ainsi,

la saisonnalité module les apports et les pertes de Hg et MeHg notamment via son influence sur l'hydrologie.

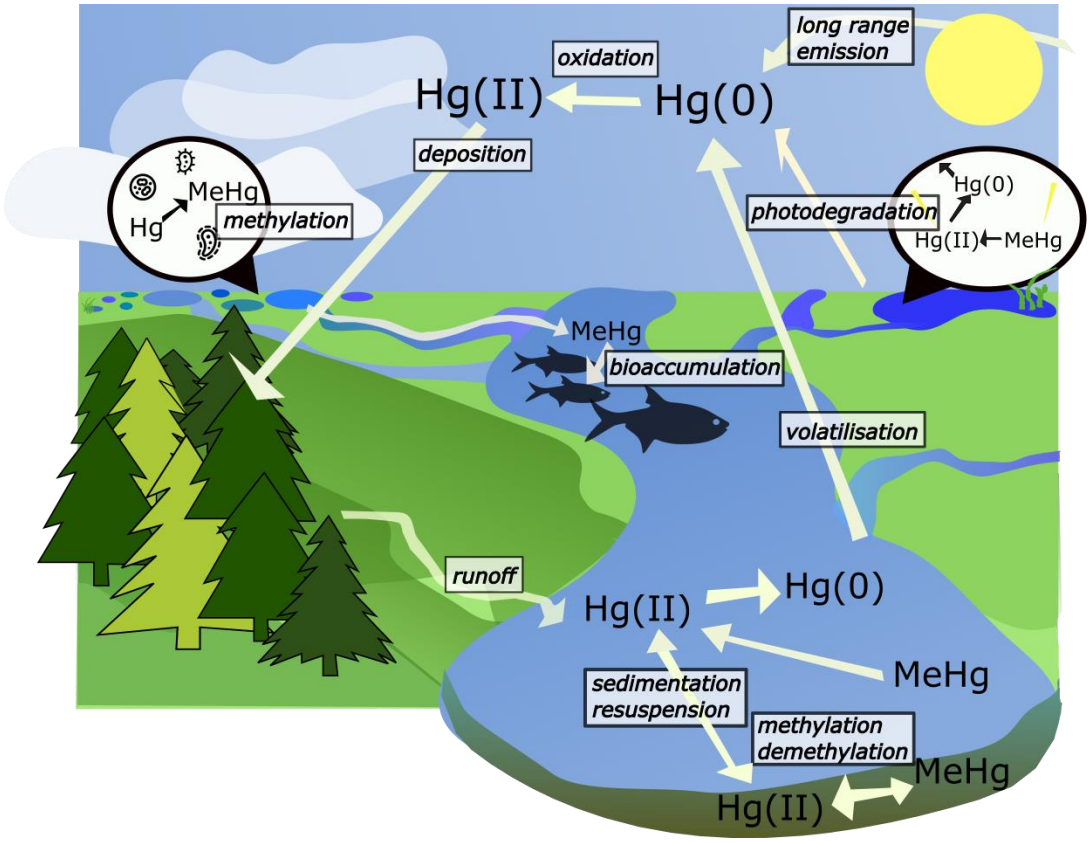

Figure 0.1. Schéma conceptuel du cycle du mercure inspired by Engstrom et al. 2007

0.2 Le paysage comme indicateur de sources et de puits

Certains éléments du paysage sont des zones sensibles pour les apports, les pertes et les transformations du Hg. Ces zones représentent des proxys potentiels pour estimer

les concentrations aquatiques, pouvant ainsi permettre d'estimer les concentrations de Hg dans les grandes rivières nordiques lorsque l'échantillonnage de ces rivières n'est pas possible. Ainsi, de nombreuses études se concentrant sur les lacs (Selvendiran et al., 2009; St. Louis et al., 1996), de petits bassins versants (Shanley et al., 2005) ou un transect de sites dans un unique bassin versant (Selvendiran et al., 2008b) ont lié positivement l'abondance en milieux humides aux concentrations de MeHg, et parfois aux concentrations de Hg. Les milieux humides sont des sources de MeHg puisqu'ils présentent généralement des zones d'anoxie et des conditions réductrices nécessaires à la production de MeHg (Benoit et al., 2002). Ils ont également été identifiés comme source de Hg (Brigham et al., 2009) puisque les milieux humides exportent typiquement du COD (Laudon et al., 2011) qui est un lien important de transport du Hg (Grigal, 2002). Les bassins versants forestiers ont aussi été associés à des concentrations terrestres et aquatiques élevées en raison de leur rôle de catalyseur dans le transfert du Hg atmosphérique, vers les sols puis vers les eaux de ruissellement (Fleck et al., 2016; Graydon et al., 2008; Obrist et al., 2016). À l'opposé, l'aire de recouvrement de lacs a été négativement liée aux concentrations de Hg et MeHg dans les lacs se retrouvant dans différents biomes (Richardson et al., 2020) et des rivières ayant de petits bassins versants (Burns et al., 2012a; Selvendiran et al., 2009). Les lacs sont considérés comme des sites de réactions, où le temps de rétention de l'eau et l'exposition au soleil sont élevés, augmentant les pertes par sédimentation ainsi que celles par photodégradation, particulièrement dans les eaux riches en COD (Girard et al., 2016; Richardson et al., 2020; Selvendiran et al., 2009). Bien qu'ils ont été reconnus

comme des sites de production de MeHg, les lacs sont également des sites de hauts taux de photodégradation, où ces pertes peuvent représenter jusqu'à 80% des apports de MeHg provenant des sédiments (Hammerschmidt & Fitzgerald, 2006; Hines & Brezonik, 2007), soulignant leur rôle de puits.

Il est donc clair que certains éléments du paysage, pris individuellement, tendent à agir plutôt comme des sources ou des puits des formes de Hg influençant les concentrations. Cependant, la plupart de nos connaissances proviennent d'études dans des lacs, à l'échelle des petites rivières drainant des bassins versants de l'ordre de quelques dizaines de km^2, ou dans une unique plus grande rivière. Ainsi, l'influence des éléments du paysage sur les concentrations de Hg dans les grandes rivières, ayant de grands bassins versants traversant d'importants gradients de climat et de couverture du paysage, reste méconnue. Puisque les apports sont dépendants de la connectivité avec le milieu terrestre, qui est moins élevée dans les grandes rivières (Covino, 2017), il est probable que certaines sources terrestres de Hg importantes à petite échelle soient plus difficiles à lier aux concentrations à grande échelle. À l'inverse, il est possible que les éléments puits du paysage prennent une importance disproportionnée dans de grands bassins versants, alors que les pertes de Hg et MeHg s'accumulent le long du continuum de grandes rivières ayant des temps de résidence de l'eau élevés. Ces hypothèses n'ont cependant jamais été testées à grande échelle spatiale. Ainsi, évaluer l'importance relative des sources et des puits est primordial afin de transférer adéquatement les acquis à diverses échelles géographiques.

0.3 Le COD comme facilitateur des apports de Hg dans les écosystèmes aquatiques

Certains éléments chimiques peuvent également faciliter l'apport de Hg vers les écosystèmes aquatiques. En particulier, le COD est fortement chimiquement complexé et géographiquement associé au Hg en raison de leurs forts liens ioniques au niveau des sites sulfurés de la matière organique humique colorée d'origine terrestre, ce qui facilite leur co-transport des sols vers les systèmes aquatiques (Ravichandran, 2004; Schelker et al., 2011). Des études ont ainsi suggéré d'utiliser le COD (Dittman et al., 2009), ou des indices de l'aromaticité du COD tels que la matière organique dissoute fluorescente (Lescord et al., 2018; Vermilyea et al., 2017) ou l'absorption UV (Burns et al., 2013), comme indicateurs des concentrations de Hg dans les rivières (Ravichandran, 2004). Cependant, une récente méta-analyse par Lavoie *et al.* (2019) a révélé que la pente de la relation Hg-COD est hautement inconstante entre les études, indiquant des ratios Hg:COD variables même lorsque les sites sont géographiquement proches. Les estimations des concentrations aquatiques de Hg à partir des concentrations en COD, basées sur l'assomption d'un couplage égal et constant, sont donc hautement imprécises. Bien que les relations avec le COD aromatique soient meilleures comparativement au COD global, puisque le Hg serait davantage lié à cette fraction du COD, ces relations varient également entre les études et les saisons (Burns et al., 2013; Lavoie et al., 2019). Ceci suggère que les facteurs environnementaux qui

modulent la relation Hg-COD sont nombreux et que des facteurs déterminants différents du transport avec le COD contrôlent les patrons de Hg dans les rivières.

En plus de la mobilisation avec le COD, les processus de pertes et transformations influencent les concentrations en Hg. Un couplage faible a d'ailleurs été associé à une pression accrue des processus de pertes dans le paysage. Par exemple, une diminution du couplage a été associé au transit dans les lacs le long du continuum aquatique (Schelker et al., 2011) et une diminution du ratio Hg : COD a été observée avec l'augmentation du temps de rétention de l'eau (Richardson et al., 2020). Plus précisément, ces différences dans le couplage ont été attribuées à l'effet des processus de pertes par sédimentation et photodégradation, qui sont accentuées avec davantage d'exposition au soleil et des temps de rétention de l'eau plus longs, alors que ces pertes sont fort probablement exercées à des taux différentiels pour le Hg et le COD (Richardson et al., 2020; Schelker et al., 2011). Dans la même perspective, des processus menant à la production de COD autochtone (i.e. produite dans les milieux aquatiques) et qui n'est pas lié aux apports terrestres de COD et Hg pourraient tendre à réduire leur couplage, ce qui pourrait expliquer pourquoi des relations plus fortes ont été observées entre la matière organique colorée d'origine terrestre et le Hg comparativement aux relations entre le Hg et le COD total (Lavoie et al., 2019). Similairement, les concentrations en MeHg ont tendance à suivre les patrons de COD lorsqu'ils proviennent tous les deux du bassin versant, tandis que le COD d'origine autochtone a été lié à des taux de méthylation élevés (Bravo et al., 2017), résultant

potentiellement en un couplage entre le MeHg et le COD autochtone, mais pas nécessairement avec le COD total. Ce couplage entre le MeHg et le COD, tout commeu celui entre le Hg et le COD, mérite une attention particulière puisque les ratios MeHg : COD aquatiques peuvent servir d'indicateur de sensibilité des écosystèmes, avec davantage de bioaccumulation dans les organismes lorsque les ratios sont élevés (Chételat et al., 2018). Les ratios MeHg : COD sont cependant également grandement variables (Lavoie et al., 2019) compliquant ainsi l'identification des endroits et moments importants de bioaccumulation. Globalement, il semblerait que le Hg, le MeHg et le COD tendent à être transportés ensemble des écosystèmes terrestres à aquatiques, mais que les processus biogéochimiques favorisant les pertes et transformations semblent favoriser leur découplage.

Ces mécanismes opposés peuvent être influencés par des éléments géographiques du bassin versant et par la saisonnalité. Par exemple, une plus grande densité de lacs, qui augmente le temps de résidence de l'eau dans le bassin versant (Gibson et al., 2015), pourrait être liée à davantage de pertes le long du continuum aquatique se répercutant en un couplage réduit entre les formes de Hg et C. De façon similaire, les hauts débits printaniers pourraient favoriser le transport hydrologique des matériaux terrestres vers les systèmes aquatiques et tandis que les bas débits favoriseraient typiquement la rétention, les transformations et les pertes dans les systèmes aquatiques avec des conséquences sur le couplage (Covino, 2017). Considérant les variations dans la nature du COD apporté vers les systèmes aquatiques selon les saisons, dépendamment des

afflux hydrologiques et de la production primaire, la saisonnalité pourrait également se traduire en des vartions temporelles dans le couplage Hg-COD et MeHg-COD. Différents degrés de couplage selon les saisons pourraient d'ailleurs expliquer pourquoi Lavoie *et al.* (2019) ont observé un couplage plus faible pour les études temporelles. Cependant, peu d'études ont directement évalué l'influence du paysage, de la saisonnalité et de l'hydrologie sur la nature et la force du couplage Hg-COD et MeHg-COD entre autres en raison des difficultés d'obtenir des données saisonnières dans les environnements nordiques. Comprendre les dynamiques Hg-COD dans les grandes rivières requiert donc d'évaluer l'importance relative de la co-mobilisation du Hg et du MeHg avec le COD en plus des facteurs de variation géographiques et temporels afin de comprendre le couplage entre les différentes formes de C et Hg.

0.4 Objectifs et hypothèses

Une meilleure compréhension des processus d'apport et de perte du Hg dans les systèmes aquatiques nous permettrait de mieux inférer les concentrations et les flux en se basant sur l'abondance d'éléments du paysage associés à des sources ou des puits dans le paysage ou encore sur les patrons de COD. Cependant, ces mécanismes pourraient ne pas être transposables dans tous les écosystèmes aquatiques. En effet, la plupart de nos connaissances sur les sources et les puits de Hg sont tirées d'études à plus petite échelle. Ainsi, il est nécessaire de savoir comment les patrons à l'échelle

locale se transposent dans de grandes rivières, ayant de grands bassins versants très hétérogènes et davantage déconnectés des sources terrestres de Hg. De plus, bien qu'un fort couplage entre le COD et le Hg est typiquement observé en raison de leur cotransport des systèmes terrestres vers le continuum aquatique, servant ainsi d'indicateur des concentrations en Hg, de récentes études ont révélé que leur couplage est hautement variable entre les systèmes. Ces indices indiquent leur co-transport n'est pas le seul mécanisme influençant leur couplage et que d'autres facteurs dans le bassin versant et dans le réseau aquatique, telles que les propriétés géographiques et les variations saisonnières, pourraient être importants à considérer. Il est donc primordial d'explorer ce qui influence le couplage Hg-COD dans des rivières traversant de grands gradients hydrologiques et de végétation, ayant potentiellement un effet sur la composition du COD apporté dans les systèmes aquatiques ainsi que sur les processus d'apport et de pertes.

Par conséquent, le premier chapitre de mon mémoire vise à 1) déterminer quels sont les éléments du paysage qui influencent les concentrations et les exports de Hg et MeHg dans les grandes rivières nordiques. J'estime que l'importance du couvert forestier (% couverture forestière), des milieux humides (% couverture par les milieux humides) et des lacs (% couverture par les milieux aquatiques) dans le bassin versant sera corrélée avec les concentrations en Hg et MeHg. Toutefois, je crois que les puits auront une importance disproportionnée puisque les grandes rivières sont davantage déconnectées des sources terrestres, rendant potentiellement plus difficile le lien entre

les éléments sources du paysage, tels que les sols forestiers et les milieux humides, avec les concentrations *in situ*. Puisque les apports et les pertes sont modulés par la le temps de rétention de l'eau, l'exposition au soleil et la température, ce chapitre vise également à 2) explorer l'influence des saisons sur les sources et les puits de Hg.

Le deuxième chapitre de mon mémoire cherche à 1) comprendre ce qui module le couplage Hg-COD et MeHg-COD. Plus précisément, il vise à savoir comment certains éléments géographiques ou saisonniers, qui influencent notamment les conditions hydrologiques et conséquemment la balance entre le transport et les processus de pertes et de transformations, ont une influence sur les ratios Hg : COD et MeHg : COD ainsi que sur la force de leur corrélation. Puisque des plus faibles couplages et ratios ont été observés dans des systèmes ayant une plus forte pression des processus de perte, je m'attends à ce qu'il y ait un fort couplage et de hauts ratios Hg : COD lorsque le temps de rétention de l'eau est court, favorisant peu de perte. Inversement, j'estime qu'il y aura un plus faible couplage Hg-COD et MeHg-COD, quand le temps de résidence est plus long, favorisant des pertes divergentes de Hg et de COD ainsi que des taux de méthylation élevés qui ne sont pas liés à des apports équivalents en COD. Un fort couplage devrait donc être observé à la fonte des neiges, au printemps, tandis qu'un faible couplage serait mesuré en été.

Afin de répondre à ces hypothèses, j'ai effectué un échantillonnage inter-saisonnier à l'échelle régionale dans 18 grandes rivières de la Baie James, s'étendant sur un gradient latitudinal de plus de 650 km de l'Abitibi à la jonction Baie James avec

la Baie d'Hudson. Cette zone d'étude permet de couvrir un impressionnant gradient en termes de couverture du sol, de température et d'hydrologie, où plusieurs rivières sur le territoire ont été harnachées pour la production d'hydroélectricité. De plus, bien que ces grandes rivières du Nord Est du Canada couvrent une importante portion des bassins versants panarctiques, elles sont rarement échantillonnées, représentant un angle mort dans les estimations actuelles des concentrations et des flux de mercure dans cette région. Cette étude vise donc également à couvrir les lacunes importantes dans les mesures directes de Hg sur ce territoire, qui sont essentielles pour une estimation plus précise des exports par les grandes rivières arctiques et subarctiques.

1 CHAPITRE I

RIVERINE CONCENTRATIONS AND EXPORTS OF HG LINKED TO WETLANDS AND WATER COVERAGE IN LARGE NORTHERN CANADIAN RIVERS

Caroline Fink-Mercier[1], Jean-François Lapierre[2], Marc Amyot[2], and Paul del Giorgio[1]

[1] University of Quebec in Montreal, Biology, [2] University of Montreal, Biological sciences

1.1 Acknowledgments

This work was funded by Niskamoon Corporation as part of the Comprehensive Costal Habitat Research Project of Eeyou Istchee and by master fellowships from the Natural Sciences and Engineering Research Council (NSERC), from the Fond Québécois de la recherche sur la nature et les technologies and from the Ecolac NSERC CREATE training program in Lake and Fluvial Ecology. We are grateful to Niskamoon Corporation members, Cree land users and del Giorgio's lab members for their help during field campaigns and logistics, and Dominic Bélanger for his assistance during laboratory analyses. The authors declare no conflict of interest.

1.2 Abstract

Large rivers are major contributors of mercury (Hg) exports to the ocean, as they integrate processes of loading and loss occurring at the watershed level. Within a watershed, stream-scale studies have revealed that specific landscape features, as wetlands or lakes, are hotspots for Hg and methylmercury (MeHg) loading, sinks and transformations, but we still do not know how these landscape features upscale to broad-scale riverine Hg concentrations and exports at the within and cross-watershed scales along large geographic gradients. In this study, we evaluate how landscape metrics (vegetation types, wetland cover, contribution of lakes, climate, hydrology) are related to concentrations and exports of Hg and MeHg in 18 large boreal rivers draining watersheds that range from 44 km^2 to 209 453 km^2, distributed along a 650 km latitudinal transect in the James Bay region of Québec. Our results underscore the role of wetlands as sources of MeHg, but further show that surface coverage of water in the watershed is the major driver of both Hg and MeHg concentrations and exports at the whole network scale. Our findings also demonstrate that seasonality modulates the relationship between landscape features and the various Hg forms. Based on hydrometric data, we additionally estimate annual exports for the whole Eastern James Bay to 441 kg Hg and 14.6 kg MeHg, for average yields of 1.70 g Hg km^{-2} y^{-1} and 0.060 g MeHg km^{-2} y^{-1}. Our study provides tools to broadly predict riverine Hg concentrations and exports with only a few easily accessible landscape metrics.

1.3 Plain Language Summary

Large rivers export an important amount of Hg, a toxic metal, from land to the ocean. Quantifying these exports remains a challenge, particularly in northern environment, because of limited data availability and incomplete understanding of the factors responsible for these exports over very large landscapes with contrasting climate and land cover (e.g. abundance of vegetation, wetlands, or water). In this study, we show that high abundance of wetlands in northern landscapes is linked to elevated MeHg, the most toxic form of Hg, in 18 northern Canadian rivers distributed across a 650 km latitude gradient. Increasing abundance of lakes and reservoirs in the landscape, however, leads to lower exports of both Hg and MeHg, suggesting that aquatic ecosystems behave as a sink in the landscape, by removing large amounts of mercury as water flows from land to the ocean. We also found that, during the summer, wetlands add more MeHg while lakes remove more Hg and MeHg, meaning that the influence of the landscape is variable in time. Based on river discharge measurements, we estimated that 441 kg Hg and 14.6 kg MeHg are transported to James Bay each year. Our study is important as it quantifies mercury exports from a region with little data available, and provides tools to broadly predict the exports of Hg in northern river from geographic data that are easily accessible to scientists.

1.4 Introduction

Large rivers are major vectors of mercury (Hg) from land to the ocean (Fisher et al., 2012). Despite being often thousands of kilometers from significant human activities, northern rivers discharge about 37 000 kg Hg to the Arctic Ocean every year (Zolkos et al., 2020), which then deposit at ocean margins and impact near-shore marine organisms (Hare et al., 2008; Lockhart et al., 2005; Zhang et al., 2015). Ongoing efforts to reduce anthropogenic Hg emissions following the Minamata Convention have led to a decrease in human emissions of Hg in some countries (UN Environment, 2019). However, the thawing of permafrost and the projected increased streamflow in northern latitudes anticipated with climate change (Déry et al., 2009; Guay et al., 2015) may result in increased mobilization of permafrost stored Hg from soils to water (Schuster et al., 2018; St. Pierre et al., 2018; Zolkos et al., 2020), enhancing riverine fluxes due to the release of historically stored Hg, therefore counterbalancing emission mitigation efforts.

The degree to which a river export Hg to the sea is determined by the balance between watershed sources and sinks. In northern regions, sources of Hg are geological and from atmospheric deposition originating from anthropogenic release (AMAP/UNEP, 2013; Fitzgerald et al., 1998). When oxidized, atmospheric gaseous Hg deposits largely on the soils and vegetation within the catchment (Lindqvist et al., 1991) and reaches aquatic systems mostly by co-mobilization with dissolved organic

carbon (DOC) (Mierle & Ingram, 1991; Riscassi & Scanlon, 2011). Once within the aquatic network, Hg can be removed from the water column via sedimentation, photo-reduction or incorporated in biomass via methylation of Hg by microorganisms under the presence of organic matter and suitable temperatures, nutrients, pH conditions and anoxia (Ravichandran, 2004; Ullrich et al., 2001). Moreover, the magnitude and relative importance of these processes vary seasonally in response to changing weather and hydrology, which modulates water residence time, temperature and sunlight exposure (Sellers et al., 2001; Selvendiran et al., 2009; Shanley et al., 2005). Current evidence suggests that a combination of geographic features affect the role of watersheds as sources vs sinks of Hg, but empirical studies are lacking at broad spatial scales.

Specific landscape or aquatic features within watersheds can result in increased Hg loading, processing and loss. Studies focusing on lakes (Selvendiran et al., 2009; St. Louis et al., 1996), single watersheds (Shanley et al., 2005) or transects in a single watershed (Selvendiran et al., 2008a) often found wetlands to be positively linked to high Hg and MeHg concentrations in draining surface waters. Wetlands generally act as sources because they release DOC accumulated in peat soils to streams, for which Hg has a strong affinity (Meili, 1991), and usually have suitable conditions for Hg methylation (Shanley et al., 2005; St. Louis et al., 1996). Forested watersheds have also been positively linked to elevated terrestrial and aquatic concentrations of Hg as their canopy enhances the surface for Hg deposition (Kolka et al., 1999b; Obrist et al., 2016).

On the other hand, increased lake coverage has been linked to lower Hg and MeHg concentrations within aquatic networks when comparing individual catchments from different biomes (Richardson et al., 2020) or small individual watersheds (Burns et al., 2012a; Selvendiran et al., 2009; St. Louis et al., 1996), because the higher residence time and increased sunlight exposure in these water bodies tend to enhance losses through photoreduction and sedimentation (Richardson et al., 2020; St. Louis et al., 1996). Although it is becoming clear that multiple processes influence fluvial Hg dynamics, most studies evaluating the Hg cycle in rivers in relation to landscape features have been conducted in relatively small individual watersheds. However, the net balance of source and sink mechanisms might differ between small watersheds, with shorter water residence time and high connectivity to terrestrial systems, and larger watersheds, because these processes are highly dependent on water residence time and connectivity (Covino, 2017). Therefore, landscape features that dominate Hg dynamics at small scales might become less relevant at predicting Hg behavior in rivers draining large watersheds that are a heterogeneous mosaic of landscape features.

Past studies on riverine Hg have typically focused on either very broad extrapolations based on modelling efforts (Amos et al., 2014), or on watershed-scale efforts that focused on mechanisms driving empirical patterns based on local landscape properties (Burns et al., 2012a; Selvendiran et al., 2008a; Shanley et al., 2005). Between these two extremes lies a gap in terms of linking broad-scale riverine Hg concentrations and exports to regional patterns in climate and land-cover. In this regard,

a recent study has estimated pan-arctic Hg riverine exports based on direct measurements from 6 of the largest northern rivers (Zolkos et al., 2020), but important areas of eastern Canada still lack direct measurements, and the landscape features responsible for the geographically varying yield (Hg export per area of landscape) remain to be elucidated. In this context, we sampled 18 watersheds ranging from 44 to 209 453 km^2, distributed along a 650 km latitudinal gradient of temperature, forest cover, wetlands extent, lake abundance, soil types and hydrologic regimes within the eastern James Bay region of boreal Québec (Canada), covering over 350 000 km^2 of catchment, mostly on Eeyou Istchee traditional land. This large-scale heterogeneity is essential to include watersheds with different combinations of landscape features, in order to unravel what are the major sources or sinks of Hg driving riverine concentrations at the intra and inter basin level. This, in turn, will ultimately dictate what landscape features driving ocean exports in this region lacking riverine Hg estimates.

1.5 Materials and Methods

1.5.1 Study area

We sampled 18 rivers along the eastern shore of the James Bay (Québec) watershed spanning a 650 km latitudinal transect in the Canadian Shield. The rivers were selected

based on their hydrological importance, ranging from Strahler order 3 to 9, and based on right to access and sample in individual traplines. The most southern site is situated near a headwater lake of Harricana River in Amos, Qc (48,57º N, 78,12º W) and the most northern site on Salmon River, near the junction between James Bay and Hudson Bay (54,63º N, 79,58º W) (Figure 1.1). Most of these rivers are situated within the Cree Nation (Eeyou Istchee) territory, and sampling and field operations were carried out with full consent from local land users, in collaboration with local communities and with the engagement of Niskamoon Corporation. The region is characterized by a latitudinal gradient in temperature, tree cover, soil type, abundance of wetlands and different hydrologic patterns. The topography is characterized by low relief and flat top summits as the result of glacial erosion, which created a landscape with a large abundance of lakes, ponds and peatlands (Natural Resources Canada, 2019). The southern portion is underlain by clay sediments, which results in high particulate loads in rivers.

There has been extensive hydroelectric development in the region, and several rivers have been either dammed, or have had their discharge diverted towards a different watershed. In particular, La Grande River, the largest river in the region, has a series of dams and large reservoirs, and has also dramatically increased its discharge, with the diversion of part of the flow from Eastmain, Rupert, Sakami and Opinaca rivers in the South, and Grande Baleine and Caniapiscau rivers in the North (Déry et

al., 2016; Messier et al., 1986). These diversions started in the 1980 and approximately doubled the natural annual discharge of the river.

1.5.2 Sampling

Sampling was carried out during summer of 2018, fall of 2018, winter of 2019, spring of 2019 and summer of 2019. For each of the 18 rivers, there was a sampling site close to the mouth (but with no marine influence), and, when possible, an upstream site close to the headwaters. For some of the rivers, a third, intermediate sampling site was situated between the mouth and the upstream site. For the campaign of summer 2019, 13 sites were added in low order streams with smaller watersheds containing low total water surface, in order to assess the influence of local catchment features on the loading of Hg. These additional stream sites have a Strahler order between 3 and 4, which is lower than most of the targeted rivers at their mouth sites (Gouvernment of Quebec, 2019). They are distributed along the latitudinal gradient and connected to 9 of the larger sampled rivers (out of the 18).

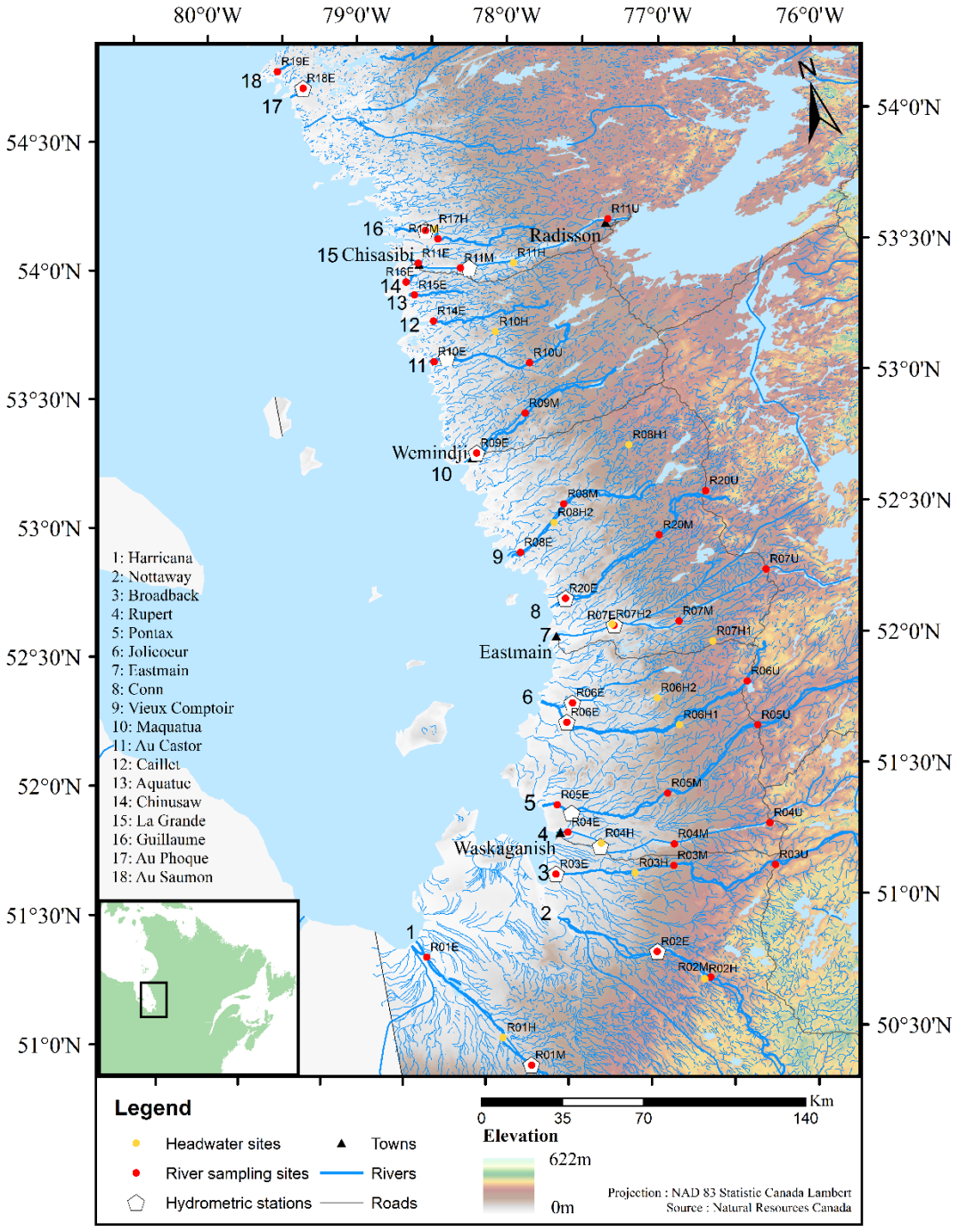

Figure 1.1 Map of the study area and the sampling sites for the 5 sampling campaigns

Due to the remote location of the sites, the majority were sampled by helicopter, mostly hovering (> 70% of samples) but also landing on water or shore when possible. Hovering did not affect the resuspension of sediments because most rivers were over 1.5 meter depth and hovering was done at a minimum of 2 meter above water, resulting in turbulence limited to surface water. Samples were collected at approximately 0.5 meter depth at all sites and pumped in a teflon tubing when hovering, limiting contact between the helicopter and sampled water. A few sites near Cree communities were sampled by boat**.** Duplicates were taken with a clean sampling protocol (Lewis & Brigham, 2004) adapted to be carried out by 1 person. For the first campaign, samples were collected in 250 mL dark borosilicate glass bottle washed with 50% acid solution (HNO_3 45%, HCl 5%) and kept cool until return to the lab. Half of the samples were filtered with 0.45 um polycarbonate filter on a Teflon filtration tower maximum 3h after sample collection. For the other campaigns, samples were collected with a peristaltic pump cleaned with HCl 10% and nanopure water between sites. Half of the samples were filtered in the field with a reusable 0.45 um polycarbonate in line filter cleaned between sites with HCl 10% and changed every 10 sites. Nanopure water and rinsed with *in situ* water. Tests were done to make sure the sampling and filtrations techniques did not induce a significative difference in concentrations. All samples were acidified with ultrapure concentrated HCl (Hydrochloric Acid, OmniTrace Ultra, Millipore Sigma™) to reach a concentration of 2% and a pH under 2 and were kept at 4°C in the dark. Duplicates of field blanks were performed on the field once every

campaign using Nanupure water running through the Teflon tube and the filtration system. Field blanks of all campaigns had a mean of 0.04 ng L^{-1} of MeHg and 0.06 ng L^{-1} of total Hg, confirming there was no contamination.

1.5.3 Mercury analyses

Mercury analyses were performed on 175 duplicates of filtered samples and duplicates of non-filtered samples. Analyses of total mercury for both filtered and non-filtered samples were conducted using a Tekran 2600 cold-vapor atomic fluorescence spectrometer (CVAFS) (Tekran® Instruments Corporation) with a detection limit of 0.05 ng L^{-1} of Hg, and following the 1631 method of the United State Environment Protection Agency (EPA) (U.S. Environmental Protection Agency, 2002). Briefly, bromine monochloride was added to samples for oxidation of all Hg form into Hg(II), and subsequently reduced with stannous chloride ($SnCl_2$) to convert Hg(II) to volatile Hg(0), collected onto gold traps and detected onto the cell of a CVAFS. Analyses of total and dissolved methyl mercury (MeHg) were conducted using the Tekran 2700 CVAFS instrument, with a detection limit of 0.01 ng L^{-1} of Hg and following the 1630 method of the EPA (U.S. Environmental Protection Agency, 2001). Samples were first distilled to remove any interference with organic matter and sulfide residues. PH was adjusted to 4.9 with acetate buffer and sodium tetraethyl borate ($NaBEt_4$) to form methylethyl mercury, then separated from solution with N_2 and collected onto a graphite carbon trap. Methylethyl mercury was ultimately carried by argon gas, converted to elemental mercury (Hg0), and detected into the cell of a CVAFS.

Instrument performance and stability were evaluated with initial and ongoing blanks and reference solutions. Analyses were repeated when chemical standards had a standard error above 10% and samples with relative standard deviation over 20% within duplicates were further examined for possible exclusion from the data set. Data in this study have a mean relative standard deviation of 3.8% for dissolved Hg (n=175 duplicates), 4.0% for total Hg (n=175 duplicates), 8.0% for dissolved MeHg (n=175 duplicates) and 9.2% for total MeHg (n=175 duplicates).

1.5.4 Geographic analyses

Spatial analyses were performed using ArcGIS 10.5. In order to delineate watersheds, flow direction and flow accumulation were derived from the digital elevation model from the Government of Canada with an altimetric precision between 4 and 12 m and a planimetric precision between 4 and 21 m (Natural Ressources Canada, 2019). For each watershed, the percentage of the different land covers, including water, wetlands of various types (forested wetlands, treed wetlands, wetlands, wetlands with shrubs, wetlands with herbs, all wetlands combined), forests, grasslands, croplands, roads, settlements and others (barren land, rocks or ice), was determined using the Land Use 2010 dataset with a spatial resolution of 30 m and an overall accuracy of 92.7% (Agriculture and Agri-Foods Canada, 2015). Watershed area was calculated using Albers conical equivalent projection.

1.5.5 River discharge and Hg export

Hydrometric stations were installed in 2018 and 2019 on 9 rivers the closest to river mouth without being influced by tides to record hourly discharge. Together with the historical hydrometric stations deployed by Hydro Québec, a total of 14 of the sampled rivers are instrumented (Figure 1.1). A pressure gauge at the stations records every hour the height of water column which is transposed into discharge with the appropriate calibrations considering the bathymetry of the river and the water velocity. Calibrations were performed at least at 4 different discharge levels to capture different water height as well as during the winter to account for the effect of ice on the pressure gauge (DeMelo et al. in prep).

Using historical and new hydrometric stations on rivers of the James Bay watershed, an annual discharge model was built with all daily year-round data available, excluding data from the dammed La Grande River to avoid the influence of this highly hydrologically impacted river on the model (DeMelo et al. in prep). Historical hydrometric data was obtained from the HYDAT data base (Government of Canada, 2020b) as well as provided by Hydro Quebec in the case of dammed rivers. Measurements from new hydrometric stations were obtained through Hydro Quebec after data validation. The model is based on the relationship between mean annual discharge and watershed area (DeMelo et al., in prep). The equation of the model was defined by fitting a linear model in R.4.0.2 (equation: $Q= 10^{-}4.78+1.08*\log(\text{watershed area})$, $R^2=0.99$), and validation of the model was done comparing modeled annual

discharge values and measured annual discharge values of recently installed hydrometric stations. This model enables extrapolation of mean annual discharge to non-instrumented sites, and subsequent verification confirmed that La Grande, Eastmain and Rupert rivers, whose watersheds have been modified, fit well in this model.

Seasonal contribution of river discharge was calculated using the proportion of the cumulative daily discharge for each season to total annual discharge for each river at the mouth sites where the hydrometric station is situated. When several years of daily discharge data were available, a daily mean was calculated. Data were derived from historical (Government of Canada, 2020b) and new hydrometric stations. The winter period ranges from January 1st to March 31st, Spring ranges from April 1st to June 30th, Summer ranges from August 1st to September 30th and Fall ranges from October 1st to December 31st (Déry et al., 2016). In the case of non-instrumented rivers, an average seasonal contribution to annual discharge of the rivers of James Bay watershed for which we have historical and present data was applied.

These seasonal discharge patterns were used to calculate seasonally weighted total annual river Hg fluxes. Seasonal concentrations were weighted based on contribution of seasonal discharge to annual discharge. The sum of the contributions was then multiplied by annual discharge to obtain annual exports. In the cases of rivers for which there were missing seasonal Hg or MeHg values, as it is the case for some

entirely frozen river during the winter, concentrations were weighted based on the remaining seasons for which Hg and MeHg data are available, and subsequently multiplied by annual discharge to obtain annual export. Hg and MeHg yields were then calculated by dividing the total annual export at the mouth by the corresponding watershed area. Export for all unsampled rivers combined were estimated using the mean, the upper limit and lower limit of Hg and MeHg concentrations of all seasons combined found in sampled rivers, multiplied by the modeled discharge based on watershed area.

1.5.6 Statistical analyses

Statistical analyses were conducted on Hg and MeHg concentrations separately because preliminary investigations showed that they do not strongly co-vary (Figure S1). Since total and dissolved forms are highly correlated (Figure S2), for simplicity all subsequent analyses were conducted on total forms only of both Hg and MeHg. To select a subset of relevant landscape variables driving Hg and MeHg ambient concentrations, elastic net regressions were performed using “ensr” package version 0.1.0 (DeWitt, 2019) in R 3.6.1 (R Core Team, 2019) using linear regression and minimizing mean cross validation error. The elastic net regression combines lasso and ridge regression penalties to help mitigate collinearity and produce a more accurate model of complex data. Seasonal discharge, area, temperature as well as relative surface area (%) of water, wetlands of various types (forested wetlands, treed wetlands, wetlands, wetlands with shrubs, wetlands with herbs, all wetlands combined), forests,

grasslands, croplands, roads, settlements and others (barren land, rocks or ice) were included as variables. For both Hg and MeHg concentrations, a log transformation was applied to normalize the residuals. For similar mean cross validation error, the most parsimonious model was selected. The R^2 of the best models were calculated using the squared correlation of concentrations predicted by the model and the real concentrations.

The variables that emerged as significant from the elastic net analysis were plotted individually to explore the shape and the strength of their relationships with Hg or MeHg concentrations, and the potential effect of seasons at the inter-watershed level. Mixed models in "lme4" package version 1.1-27.1 (Bates, 2010) were constructed to evaluate individual relationships considering spatial autocorrelation of sampling points within rivers. Seasonal effects were tested on landscape variables allowing for both different slopes and intercepts depending on season. Because visual interpretation suggested that the 13 additional small watershed sites that we sampled once in 2017 seemed to be differently responding to % water in relation to total Hg, these sites were removed from analyses involving total Hg and % water and these models were recalculated. In the model involving MeHg and % water, the northernmost site (35% water) was excluded from the model but still reported on the plots due to the high leverage of this site on the regression. Its removal allows for a fit that better represents the average of the sites, but the relationship remains significant if it is not removed. All residuals of the selected mixed models were further examined to ensure they meet the

assumptions. In the case of log-transformed data, a log-transformed curve was fitted rather than a linear curve on log-transformed values to better compare the shape of the distributions and the concentrations depending on landscape drivers and seasons.

Intra-watershed level relationships were evaluated by calculating differences in landscape properties and Hg forms (Δ) between pairs of sites of a same river. Upstream values of watershed properties were subtracted to downstream values to calculate Δ % watershed feature. The same was done for concentrations of Hg and MeHg to calculate Δ concentrations of Hg and MeHg. Relationships between Δ % watershed property and Δ concentrations of Hg and MeHg were evaluated for the same landscape features as for the inter-watershed mixed models. This approach enabled us to compare shifts in Hg related to landscape elements without spatial autocorrelation issues. Chi-square tests were performed to evaluate if points followed a distinct pattern or were randomly distributed among quadrants.

Yields of Hg and MeHg for sampled rivers were calculated using cumulative flow-weighted concentrations multiplied by annual discharge and reported by km^2. Yields were plotted against the most relevant landscape feature in the watershed (here % water) as a mean to evaluate the propensity of a watershed to export. Linear regression models were tested, and underlying assumptions were validated. Alpha level for significance was set to 0.05 for all statistical analysis.

1.6 Results

1.6.1 Spatial and seasonal patterns in Hg concentrations and exports

Hg concentrations in the sampled rivers ranged from 0.46 to 7.59 ng L^{-1}, with the lowest concentrations during winter and highest during summer, the latter in a small stream site (Table 1.1). MeHg ranged from 0.03 to 0.48 ng L^{-1} also with the highest concentration during the summer. Watersheds exhibited large variation in landscape properties (Table 1.1), namely in area from 44 to 209 453 km^2 and mean annual discharge from 0.49 to 3446 $m^3 s^{-1}$, resulting in large differences in exports and yields across watersheds. Export of total Hg was highest in Nottaway River (177 kg Hg y^{-1}) which interestingly has the second largest watershed, well under that of La Grande River (85.77 Hg y^{-1}). Export of MeHg was highest in La Grande River (5.79 g MeHg km^{-2} $year^{-1}$), which nevertheless has the lowest yields of both Hg (0.41 g Hg km^{-2} $year^{-1}$) and MeHg (0.028 g MeHg km^2 $year^{-1}$) of all sampled rivers.

Table 1.1 Summary of watershed properties, concentrations, exports and yields in the 18 sampled rivers of Eastern James Bay

River	MeHg (ng L^{-1})		Hg (ng L^{-1})		Watershed area (km^2)		Annual discharge ($m^3 s^{-1}$)		Water (%)		Forest (%)		All Wetland (%)		Export MeHg (Kg y^{-1})	Yield MeHg (g $km^{-2} y^{-1}$)	Export Hg (Kg y^{-1})	Yield Hg (g $km^{-2} y^{-1}$)
Chinusaw	**0.23**	(0.16-0.28)	**3.5**	(2.78-3.87)	**44**		**0.5**		**6.4**		**45.7**		**43.2**		**0.0033**	**0.075**	**0.055**	**1.24**
Salmon	**0.15**	(0.12-0.16)	**1.33**	(0.78-2.70)	**68**	(68-69)	**0.8**		**34.9**	(34.5-35.1)	**9**	(9.0-9.1)	**18.3**		**0.0034**	**0.050**	**0.043**	**0.63**
Aquatuc	**0.27**	(0.12-0.36)	**4.11**	(3.87-4.39)	**188**		**2.3**		**5.4**		**53.7**		**22.9**		**0.018**	**0.094**	**0.30**	**1.59**
Caillet	**0.17**	(0.09-0.23)	**4.33**	(4.25-4.44)	**470**		**6.3**		**7.2**		**50.3**		**23.9**		**0.029**	**0.063**	**0.86**	**1.83**
Guillaume	**0.18**	(0.08-0.25)	**4.02**	(3.51-5.06)	**672**	(152-888)	**13.3**	(1.9-18.9)	**5.4**	(5.3-5.9)	**53.8**	(49.8-54.8)	**15.8**	(15.1-16.9)	**0.078**	**0.092**	**2.22**	**2.62**
Conn	**0.16**	(0.07-0.23)	**3.62**	(2.65-4.73)	**691**	(108-1183)	**10.5**	(1.3-19.7)	**7.4**	(6.2-8.2)	**61.4**	(58.9-64.7)	**12.6**	(11.4-15.3)	**0.084**	**0.073**	**2.18**	**1.91**
Jolicoeur North	**0.18**	(0.10-0.25)	**4.73**	(3.03-6.67)	**783**		**10.9**		**5.5**		**52.7**		**28.4**		**0.050**	**0.064**	**1.67**	**2.14**
Jolicoeur South	**0.23**	(0.07-0.48)	**4.88**	(2.83-6.78)	**942**	(100-1777)	**13.7**	(1.2-26.4)	**3.9**	(1.3-5.7)	**56.2**	(50.8-64.5)	**25.5**	(18.7-31.4)	**0.12**	**0.069**	**3.38**	**1.90**
Maquatua	**0.09**	(0.05-0.15)	**2.81**	(2.49-3.21)	**965**	(894-1036)	**14.1**	(12.5-15.5)	**12.9**	(12.3-13.5)	**48.5**	(47.5-49.6)	**16**	(15.7-16.3)	**0.046**	**0.044**	**1.38**	**1.33**
Seal	**0.1**	(0.04-0.16)	**1.82**	(1.08-2.79)	**1508**	(1486-1575)	**34.5**		**22.1**	(22.0-22.2)	**43.5**	(43.2-43.6)	**11.5**	(11.4-11.7)	**0.1**	**0.069**	**2.21**	**1.47**
Beaver	**0.09**	(0.04-0.22)	**2.94**	(2.15-4.09)	**1860**	(109-2941)	**25.3**	(1.3-45.4)	**11.3**	(4.4-14.0)	**52.7**	(44.1-54.8)	**17.1**	(14.7-30.8)	**0.11**	**0.036**	**3.79**	**1.29**
Eastmain *	**0.12**	(0.06-0.24)	**4.01**	(2.79-6.39)	**2063**	(144-3973)	**30.3**	(1.7-58.6)	**8.5**	(1.7-10.4)	**59.1**	(48.0-62.4)	**21.5**	(17.6-37.9)	**0.14**	**0.036**	**6.54**	**1.65**
Old Factory	**0.12**	(0.06-0.24)	**3.13**	(1.92-4.76)	**2094**	(132-2723)	**32.3**	(1.6-42.8)	**8.2**	(2.0-9.6)	**51**	(41.4-55.4)	**15.7**	(12.0-31.7)	**0.12**	**0.045**	**4.11**	**1.51**
Pontax	**0.11**	(0.06-0.17)	**3.38**	(1.78-4.48)	**6150**	(4049-7894)	**99.7**	(64.1-131.9)	**5.7**	(5.3-5.9)	**51.1**	(48.8-53.6)	**25.9**	(23.4-29.4)	**0.44**	**0.056**	**14.88**	**1.89**
Rupert *	**0.07**	(0.04-0.13)	**1.47**	(0.77-2.16)	**10153**	(96-11 596)	**238.7**	(1.1-393.1)	**14.6**	(0.6-16.4)	**59.7**	(8.9-65.1)	**20.4**	(12.9-89.7)	**0.70**	**0.060**	**19.92**	**1.72**
Broadback	**0.08**	(0.05-0.19)	**3.54**	(2.54-4.95)	**17356**	(171-20 868)	**328.7**	(2.1-421.6)	**12.6**	(0.5-14.6)	**65.6**	(51.4-69.0)	**19**	(15.5-31.1)	**0.98**	**0.047**	**49.9**	**2.39**
Harricana	**0.13**	(0.10-0.17)	**3.75**	(1.93-6.33)	**17836**	(224-29 418)	**325.4**	(2.8-546.0)	**5.5**	(2.6-9.4)	**66.8**	(23.6-74.1)	**23.9**	(11.5-72.8)	**1.97**	**0.072**	**65.71**	**2.40**
Nottaway	**0.11**	(0.09-0.15)	**4.82**	(3.88-7.59)	**55105**	(109-62 159)	**1081.9**	(1.3-1224.7)	**9.5**	(4.7-10.1)	**74.5**	(46.9-77.7)	**15.4**	(11.5-48.4)	**3.92**	**0.064**	**177.21**	**2.89**
La Grande *	**0.07**	(0.03-0.24)	**1.11**	(0.46-3.27)	**189880**	(220-209 453)	**3133**	(2.8-3446.0)	**22.2**	(2.7-24.3)	**56.5**	(46.7-57.5)	**7.4**	(5.7-23.8)	**5.79**	**0.028**	**85.77**	**0.41**
All rivers	**0.12**	(0.03-0.48)	**3.27**	(0.46-7.59)	**21781**	(44- 209 453)	**380.8**	(0.49-3446.0)	**10.6**	(0.5-35.1)	**56.4**	(8.9-77.7)	**19**	(5.7-89.7)	**0.78** (0.003-5.79)	**0.060** (0.028-0.094)	**23.27** (0.055-177.21)	**1.70** (0.41-2.89)

Note. Rivers marked with * are rivers that have either been diverted (Rupert and Eastmain rivers) or regulated for hydropower (La Grande river). Bold values represent the mean river value for all sites within the river (upstream, middle, downstream, small stream site) and values in brackets represent the minimum and maximal values considering all sites within the river. Rivers with landscape properties without intervals have only 1 site within the river. Yields and exports were calculated at the mouth only (1 value per river). All Hg and MeHg concentrations presented are average of duplicates. Watershed area represent the drainage basin at sampling points. % Water refers to area covered by water in the watershed and % All wetlands refers to area covered by all wetland types combined (see methods for wetland types) in the watershed.

1.6.2 Cross-river drivers of Hg concentrations

Out of the 16 metrics included in the elastic net regressions, only 3 were selected in the elastic net model for MeHg that were run with all the data (R^2= 0.69) (Table 1.2). Relative freshwater area (percent water) and relative forested area (percent forest) in the catchment had a negative impact on river MeHg concentrations, whereas percent wetlands (all types combined) had a positive effect. Only two landscape metrics, were selected for the Hg model (Table 1.2) with a R^2 of 0.66. Percent water in the catchment also had a negative effect on Hg concentration, whereas contrary to the MeHg model, percent forest had a positive effect, and percent wetlands was not included.

Table 1.2 Elastic net regression coefficient from Hg and MeHg concentrations models including all sites and all seasons

Model	Landscape metrics	Coefficient	R^2
Total MeHg	Intercept	-1.49	0.69
	% Water	-0.028	
	% Forest	-0.0087	
	% All Wetlands	0.0017	
Total Hg	Intercept	1.47	0.66
	% Water	-0.046	
	% Forest	0.0015	
	% All Wetlands	n.s	

The mixed models were used to assess the potential effect of seasonality and the associated hydrologic shifts, on individual landscape relationships with Hg and MeHg. This analysis revealed that percent water and seasons together explained 78% of the variance in seasonal MeHg concentrations (Figure 1.2b, Table S1). Summer and fall had steeper regression slopes between MeHg and %water compared to the slopes of winter and spring (Figure 1.2b, Table S1). Percent wetlands and seasons together explained 68% of the variance in MeHg concentrations (Table S1). Three sites in different rivers with a very high proportion of wetlands (48%, 73% and 90%), which correspond to sites in smaller streams that were added in the last sampling campaign, were clear outliers (Figure 1.2c) as confirmed by Cook's distance diagnostic plot of the residuals of the model. To avoid a disproportionate weight of these sites in the model, these sites were excluded from the regression analysis. In this model, slopes for the summer and fall were steeper compared to the ones for winter and spring (Figure 1.2c, Table S1), suggesting that the loading influence of wetlands on riverine MeHg is much stronger during summer and fall. In the mixed model considering percent forest and seasons, the variance was mostly explained by the random effects ($R^2m=0.19$, $R^2c=0.72$) and the model was not significant (Table S1, Figure 1.2d), implying that percent forest has little influence on MeHg concentrations, whereas the river unit (random effect) explains much of the difference in concentrations.

In the case of total Hg, percent water and percent forest relationships were explored with mixed models. Percent water and seasons explained 74% of the variance

in riverine Hg when the small stream site, for which we did not have seasonal data, were excluded. This model shows a slightly lower slope during spring compared to summer and fall, although this difference is not significant (Figure 1.2a, Table S1). The variance of mixed model based on percent forest and seasons was almost entirely explained by random effects ($R^2m=0.078$, $R^2c=0.81$), and the model was not significant (Table S1), which implies that percent forest and seasons alone have little influence on Hg concentrations. However, when combined with percent water, it might explain some more variation not explained by the water, as it was a significant predictor in the elastic net regression.

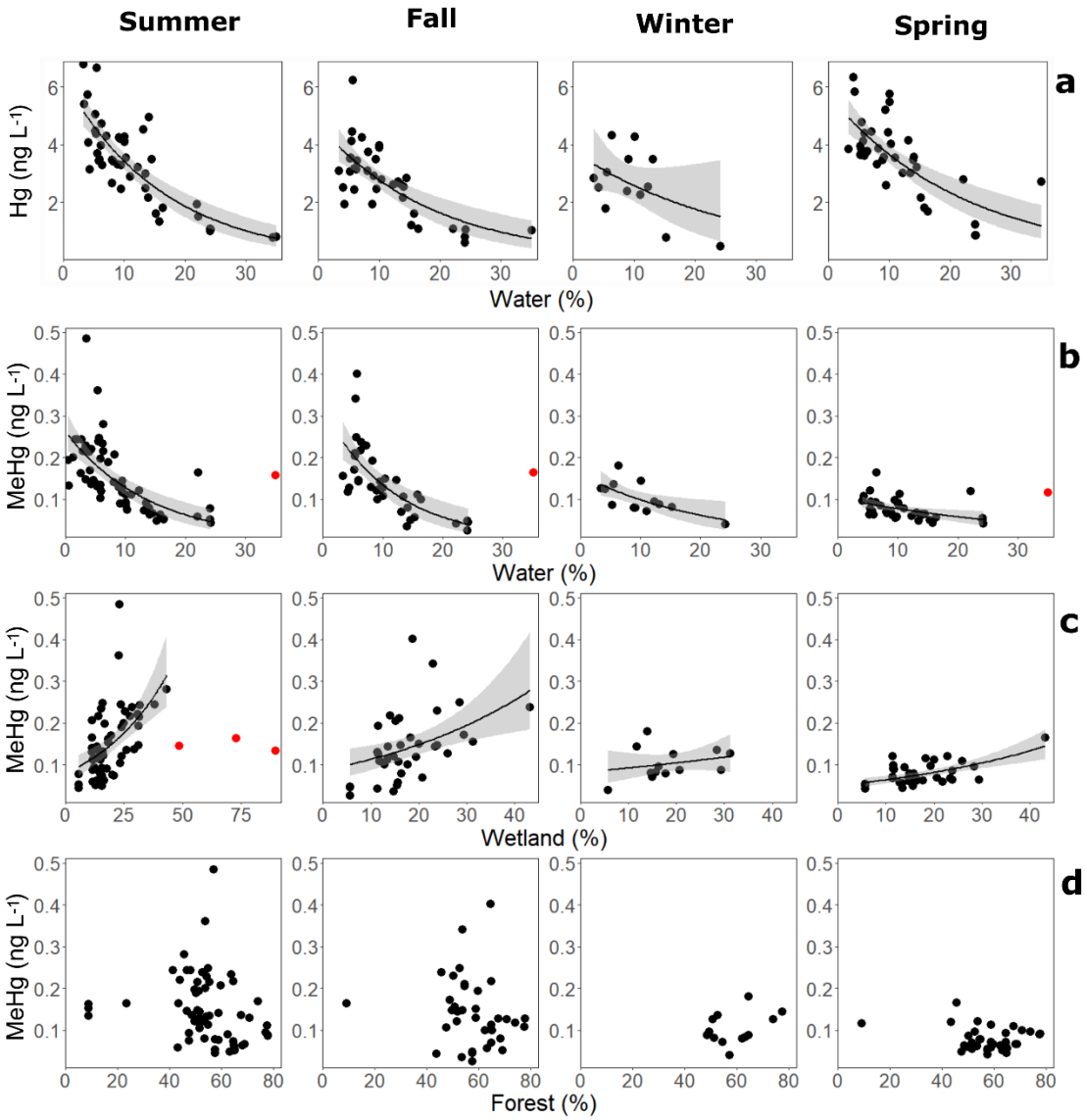

Figure 1.2. Hg and MeHg concentrations relationships with landscape features by seasons (n=175). a) Hg concentrations as a function of % water b) MeHg concentrations as a function of % water c) MeHg concentrations as a function of % wetland (all types) d) MeHg concentrations as a function of % forest. Red dots represent sites that were excluded from the regression due to very high leverage. Grey areas represent standard error around the curve. R^2 and p-values of the models are shown in Table S1.

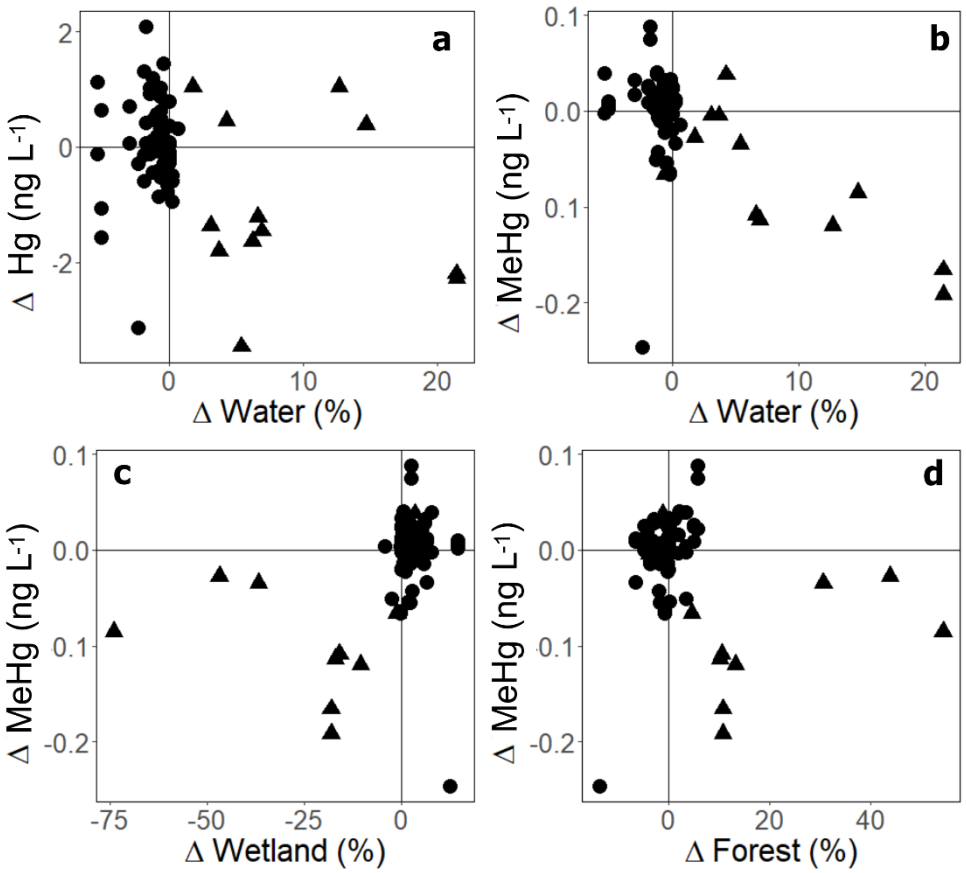

Figure 1.3. Change in Hg (Δ Hg) and MeHg (Δ MeHg) concentrations as a function of the change in landscape metrics within rivers. a) Δ Hg as a function of Δ % water, b) Δ MeHg as a function of Δ % water, c) Δ MeHg as a function of Δ % wetland (all types), d) Δ MeHg as a function of Δ % forest. Triangles represent small stream sites that were sampled once.

1.6.3 Within-river patterns of Hg concentrations

The patterns described above explain how cross-system differences in landscape properties are associated with cross-system differences in Hg concentrations. In order to explore whether these patterns hold at the within-river scale, and to avoid

spatial auto-correlation within rivers, we calculated the change in Hg concentrations between sites within a given river (Δ Hg concentrations), and related this to the change in landscape features between the corresponding portions of the watershed (Δ landscape feature), and we assessed to what extent a change in a given landscape property resulted in a change in Hg (or MeHg) concentration within the watershed. Delta pairs were between 1 km and 100 km apart (Figure 1.1). We found that overall, small changes in land cover did not lead to consistent responses in terms of Hg and MeHg concentrations within the river, but that pairs of sites that had large differences in landscape properties did have consistent shifts in Hg and MeHg concentrations (Figure 1.3). The greater shifts were more evident with the addition of small river sites, which greatly expanded the range in both landscape metrics and Hg and MeHg concentrations eventhough they were not systematically further from their paired sites compared to larger river site pairs (Figure 1.1). The delta Hg generally responded to changes in land cover in ways that were coherent with cross system patterns: a decrease in MeHg and Hg with an increase in % water and an increase in MeHg with an increase % wetlands within the watershed, with very few points found in a quadrant that contradicts the observed cross-system patterns (e.g. top-right quadrant in Figure 1.2a would imply that gaining water in sub-watersheds would lead to increasing concentrations of Hg). The khi-square test revealed that the distributions of points in the relationships involving % water and Hg (Figure 1.3a), % water and MeHg (Figure 1.3b) and % wetland and MeHg (Figure 1.3c) are highly significantly different from a

random distribution that would expect that each quadrant should contain about 25% of the pairs of sites (Table S2), suggesting that a gain in % water reduces Hg and MeHg riverine concentrations and that a gain in % wetlands increases MeHg concentrations. The relationship considering changes in % forest and MeHg concentrations did not have a distribution of points significantly different from an even distribution (Table S2), suggesting little influence of % forest on MeHg concentrations.

1.6.4 Riverine yields of Hg as a function of watershed properties

The Hg fluxes presented in Table 1.1 resulted in catchment-specific yields that varied from 0.41 to 2.89 g km^{-2} y^{-1} for total Hg, and from 0.028 to 0.094 g km^{-2} y^{-1} for MeHg (Table 1.1). Percent water in the catchment was by far the strongest predictor of Hg and MeHg concentrations, and consequently, it was a relatively strong predictor of yields as well (Figure 1.4). More specifically, percent water explained 26% of the variance in MeHg yields ($p = 0.018$), and 50% of the variance in total Hg yield ($p = 0.00043$); both relationships were negative, implying that watersheds with high water density tend to export less Hg per km^2 compared to watersheds with low water density. Conceptually, the intercept of these models represents the expected yield if there was no water in these catchments, presumably reflecting the export from soils and wetlands before the influence of lake- and reservoir-mediated sinks. Based on this reasoning, we estimate that on average each km^2 of catchment in our study area exports about 2.52 g Hg km^{-2} yr^{-1} (confidence interval: 1.91-3.33 g Hg km^{-2} yr^{-1}) and 0.078 g MeHg km^{-2} yr^{-}

[1] (confidence interval: 0.059-0.10 g MeHg km^{-2} yr^{-1}) to the aquatic network, and that cross-system differences in yield at the mouth of these fluvial networks are explained by gradual losses in surface waters within the catchments.

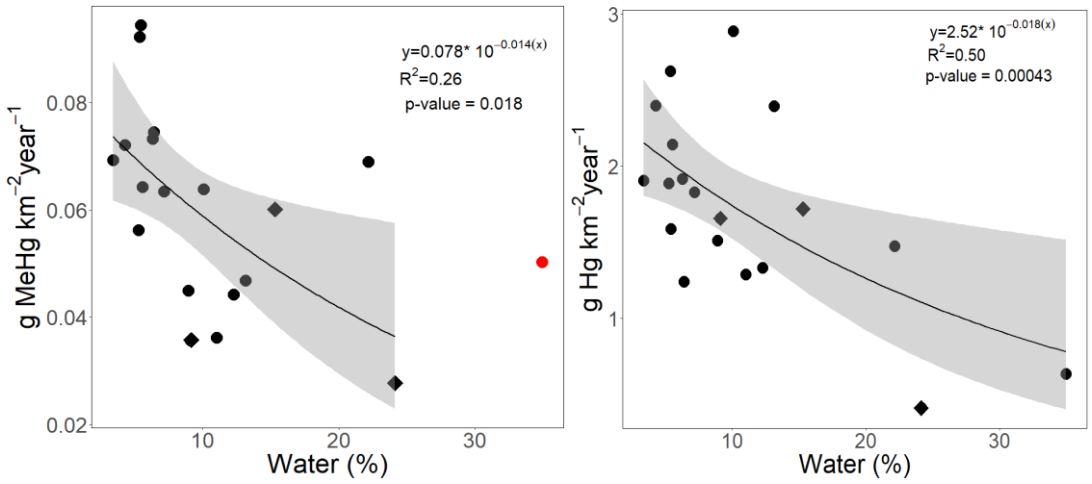

Figure 1.4. Annual yields of Hg and MeHg per km^2 of watershed as a function of % water in the watershed. Exports were calculated using the mean annual discharge at the mouth of each river. The red dot represents a site (Salmon River) excluded from the regression due to very high leverage. Grey areas represent the standard error around the curve.

1.7 Discussion

In this study, we show that northern rivers in the James Bay region of boreal Québec have comparable (yet in the lower range) Hg and MeHg concentrations to other northern rivers, and that concentrations and exports can be explained by geographic properties such as percent wetlands, forests and water in the catchment. In particular,

we measured concentrations ranging from 0.46-7.59 ng Hg L^{-1} and 0.03-0.48 ng MeHg L^{-1} (Table 1.1). This compares well with average annual concentrations found in major Canadian northern rivers [0.9-7.2 ng Hg L^{-1} and 0.08-0.2 ng MeHg L^{-1}, (Schuster et al., 2011)] and with pristine lakes and rivers of the boreal Canadian Shield [0.32-7.4 ng Hg L^{-1} and < 0.004-0.31 ng MeHg L^{-1} (Lescord et al., 2018; Schuster et al., 2011; Sellers et al., 2001)], although the concentrations found in our study are not fully comparable to major Arctic rivers [5.6-14.9 ng Hg L^{-1} and 0.05-4.90 ng MeHg L^{-1} (St. Pierre et al., 2018; Zolkos et al., 2020)], which can have much higher values of Hg and MeHg due to elevated concentration of particles and to permafrost thaw and associated erosion. These large differences in concentrations emphasize the importance of assessing Hg patterns in eastern Canadian northern rivers for accurate estimation of global aquatic Hg flux to the Arctic ocean. Moreover, we found that the concentrations in the James Bay rivers are largely driven by differences in water and wetland coverage across watersheds (Figure 1.2); rivers in watersheds with high percent wetlands tended to have high MeHg concentrations whereas rivers in watersheds with higher percent water tended to have lower Hg and MeHg concentrations. These same landscape properties explained differences at the within river scale (Figure 1.3), although the coupling between the Hg species and landscape properties was much weaker at the intra-river scale than across watersheds.

1.7.1 The watershed drivers of Hg concentrations in pristine boreal rivers

Previous studies had identified wetlands as the most important landscape driver of MeHg concentrations in fluvial networks (Brigham et al., 2009; Grigal, 2002; Kirk & St. Louis, 2008; Kolka et al., 1999a; St. Louis et al., 1996) whereas in our large scale study, surface water density in catchments emerged as the primary driver of both Hg and MeHg concentrations. At both the inter-basin and intra-basin levels, Hg and MeHg concentrations tend to decrease with increasing proportion of water surface in the basin, although lower-order streams exhibiting larger differences in landscape properties had to be included in order to detect a change in concentrations at the intra-basin level. These results are consistent with other studies that have demonstrated the importance of lakes as potential sinks of Hg (Burns et al., 2012a; Selvendiran et al., 2009). High surface water relative coverage within the watershed and the ensuing longer water residence time (Gibson et al., 2015) lead to longer exposure to sunlight, both favoring photodegradation, biodegradation and sedimentation, all of which enhance the removal of different Hg species from the water column (Richardson et al., 2020; Selvendiran et al., 2009). Although lakes have also been shown to be sites of MeHg production, they are also sites of high rates of photodegradation especially in DOC-rich waters (Girard et al., 2016). Studies based on in vitro experiments have estimated that annual loss by photodegradation under light exposure similar to conditions in our study area can account for 80% of the MeHg mobilized annually from in situ sediment production (Sellers 2001, Hammerschmidt and Fitzgerald 2006), highlighting the importance of

in-lake photodegradation in MeHg cycling. The removal of Hg could also be partially due to remobilization in biota which can represent a significant in-lake loss (Hines & Brezonik, 2007). Therefore, we interpret the negative relationship between concentrations of mercury and percent water in the landscape as a removal effect in response to increasing water residence that enhances the loss of Hg forms through multiple biogeochemical pathways (Figure 1.2, Table 1.2), as lakes are recognized as regulator of downstream exports via retention (Lepistö et al., 2006; Tranvik et al., 2009). The increase in water coverage could also represent a loss of land proportion in the watershed, and therefore a loss of Hg from terrestrial inputs that could potentially explain the lower Hg and MeHg concentrations in watersheds with higher %water. However, if atmospheric deposition is the dominant ultimate source of Hg, it should still deposit, although directly on surface water instead of on land, resulting in no loss of Hg inputs. Hence, we argue that the removal effect of lakes is the main mechanism responsible for the lower Hg and MeHg concentrations in watersheds with higher proportions of surface waters. At the inter-basin level, the relationship was modulated by seasonal differences in hydrology and temperature, with higher average MeHg concentrations during summer and fall and also a steeper slope for both Hg and MeHg versus percent water. Steeper slopes for MeHg compared to Hg during summer and fall show that MeHg is removed faster from the water, therefore decreasing %MeHg as water coverage increases in the watershed. A similar pattern was reported by Richardson (2020) for lakes, where there was a decrease in % MeHg with increasing

water residence time. Water coverage in the watershed is therefore the primary driver of Hg and MeHg dynamics in the fluvial network, influencing the net sink and source balance.

The proportion of wetlands in the watershed also emerged as a significant driver of MeHg concentrations (albeit not of total Hg), both across and within rivers, although the intra-river pattern was only detectable when a set of smaller rivers in order was considered, potentially due to the lower geographical classification accuracy of wetlands (84.8%) (Agriculture and Agri-Foods Canada, 2015), incorporating variation in the model. Nervertheless, MeHg concentrations tended to increase with wetland coverage especially during summer and fall seasons (Figure 1.2). This is consistent with previous smaller scale studies that highlighted the importance of wetland environmental conditions, including pH, anoxia and redox gradients that favor the formation of MeHg, particularly during the summer and fall when temperatures are higher, water residence times longer (Selvendiran et al., 2008a; Shanley et al., 2005). On the other hand, conditions in spring, with lower water temperatures and high flushing rates, do not favor the accumulation of MeHg compared to summer and fall, highlighting that seasons modulate the amplitude of the loading of MeHg from wetlands. balancing this landscape source of MeHg.

Forest cover also emerged as a driver of both Hg and MeHg concentrations, albeit a much weaker one relative to water coverage in the watershed (Table 1.2, Table S1).

The negative effect of forest cover on MeHg (Table 1.2) is in agreement with previous studies that have reported that MeHg tends to be retained and demethylated in upland forest catchments because of the prevailing aerobic conditions, favorable for demethylation of MeHg that was formed under previous anaerobic conditions (St. Louis et al., 1996). In contrast, the relationship between forest and Hg was positive, albeit weak (Table 1.2, Table S1). This weak relationship, despite emphasis of previous studies on the pivotal role of forests in transferring atmospheric Hg to soils and subsequently to aquatic systems (Grigal, 2002; Obrist et al., 2016), suggests a minor influence of forests in driving Hg inputs in these large boreal large watersheds. This may be due to the weaker connectivity to land compared to smaller watersheds, resulting in forest influence being overwhelmed by removal processes independent of land connectivity. Unfortunately, the land use model did not incorporate deforestation or burned forest classes, preventing us from interpreting the role of these subclasses of forest on Hg patterns. However, a burned forest area was observed in the Eastmain river watershed while sampling, yet Hg and MeHg concentrations downstream of this burned site do not seem to diverge from the models.

Overall, our results show that most landscape drivers that have previously been identified at more local scales allow us to explain regional, cross-river, as well as intra-river patterns in concentrations of Hg in large northern boreal rivers. We further show that, at broad spatial scales, sink processes appear to dominate over loading processes, as evidenced by the very strong importance of percent water in the catchment compared

to other drivers of Hg concentrations in these large rivers. The increasing residence time within the aquatic network promotes the loss of the various Hg forms to either sediments or the atmosphere on the way to the river mouth, decoupling the connection to land and weakening the role of terrestrial sources, including wetlands and forest cover, as drivers of riverine Hg and MeHg concentrations.

It is interesting to note that La Grande river, which is dammed, followed the same patterns as the undammed rivers (Table 1.1). In the La Grande watershed, the construction of a series of large dams has increased the total aquatic surface area within this watershed by over 200% relative to the original landscape. Although reservoirs have been reported to be sites of intense remobilization and processing of soil-derived Hg, with consequences on food web Hg and even human Hg accumulation (Mucci et al., 1995), it is also clear that this is a time-dependent process that tends to subside with reservoir age (Verdon et al., 1991). At present, La Grande has among the highest % water in its watershed of all boreal rivers, and has the lowest yield of Hg from at its mouth (0.41 g Hg km^{-2} y^{-1} and 0.028 g MeHg km^{-2} y^{-1}). The fact that it fits the overall cross-river pattern would suggest that these reservoirs, which are all over 40 years old, are no longer acting as net sources of Hg but rather as regular aquatic sinks. On the opposite end, the Eastmain and Rupert rivers have been deviated towards La Grande watershed, therefore decreasing their discharge by 88% and 27% respectively (Déry et al., 2016) and their % water to 51% and 75% of their original relative water coverage. Interestingly, Eastmain and Rupert rivers also fit the overall patterns of concentrations

and yields relative to the current percent water in their respective post-deviation watersheds. This represents a whole landscape manipulation that is almost analogous to an experimental test of watershed drivers of Hg dynamics, supporting the idea that landscapes with longer water retention times, whether it is due to increased lake volume or aged reservoir volume, will favor losses over gains of mercury along the land-sea continuum.

1.7.2 Patterns in areal exports of Hg from boreal catchments

Because water coverage is such a strong indicator of Hg concentrations at both the river mouth and along the flow path within subsections of the watershed, annual export of total Hg and MeHg to the ocean per unit landscape can be predicted from percent water in the watershed with relatively good accuracy ($R^2 = 0.50$ for Hg, $R^2 = 0.26$ for MeHg) (Figure 1.4). Only one river diverged from the distribution curve of MeHg exports (Salmon River, Figure 1.4). This river has the second smallest watershed area and is the northernmost in our study, is extremely shallow, and has a high degree of connectivity of the water column with bottom sediments which could explain the high MeHg concentration found due to methylation in the sediments (Sunderland et al., 2004). This river is also influenced by distinct landscape characteristics, including potentially discontinuous permafrost. In this case, % water was not a good predictor of MeHg concentrations suggesting that caution should be taken when using this model

to extrapolate MeHg exports in shallower rivers or northern rivers with watersheds influenced by continuous or discontinuous permafrost.

The intercept of the model, which corresponds to a scenario of 0 % water or the interface between terrestrial and aquatic systems, can be used to estimate an average land to river export across the study area, which would correspond to the areal loading of Hg in the absence of loss in the aquatic portion of watersheds. The intercepts of our export models (2.52 g Hg km^{-2} yr^{-1} and 0.078 g MeHg km^2 yr^{-1}) are remarkably close to previously reported Hg runoff yields from northern forested catchments of 2.2-2.8 g Hg km^2 yr^{-1} (Grigal et al., 2000; Larssen et al., 2008) and 0.01 to 0.33 g MeHg km^{-2} yr^{-1} (Grigal, 2002; Porvari & Verta, 2003), suggesting that this statistical approach yields to soil-water mercury export estimates that are comparable to measured fluxes, and furthermore, that these soil to water mercury exports may be relatively similar across landscapes.

Although there are surely variations in the magnitude of this land-water transfer of Hg driven by local geology and the distributions of wetlands and forests, our results suggest that on average the regional land/water flux for this boreal region is roughly 5 to 10-fold lower than Hg deposition from the atmosphere, which is estimated to be ranged from 12.4 to 25.4 g Hg km^2 yr^{-1} in these boreal landscape (Graydon et al., 2008; Muir et al., 2009). This means that a significant fraction of the deposited Hg is either volatilized or sequestered in forest soils and that only a fraction is exported to aquatic

systems. In contrast, MeHg atmospheric deposition, which in this regions is estimated to range between 0.1 and 0.2 g MeHg km^2 yr^{-1} (Graydon et al., 2008), is almost of the same magnitude as our estimate of MeHg flux from land to water, which could imply that either a larger fraction of deposited MeHg is exported to aquatic systems compared to Hg, or that aquatic MeHg dynamics is in fact less dependent on atmospheric inputs and more linked to in situ processing of Hg. The second hypothesis is more plausible; for example, the METAALICUS experiments showed evidence that newly deposited Hg is efficiently retained in soils (Graydon et al., 2012) and production in the basin has been shown to be the primary source of MeHg to streams in watersheds with wetlands (Brigham et al., 2009). Regardless, our results suggest that MeHg export from land to water is closer in magnitude to atmospheric deposition than total Hg export, and that the latter may be relatively uniform across the landscape. On the other hand, riverine export to the ocean per unit watershed at the river mouth, which are also comparable to estimates for major Arctic rivers of 0.8-4 g Hg km^{-2} y^{-1} (Zolkos et al., 2020) (Table 1.1), varied by almost one order of magnitude (Figure 1.4), but this variability was mainly driven not by cross-watershed variations in local export from soils to water, but rather by how much Hg was lost in transit within the aquatic network as a whole.

Taken together, we estimated that the sampled rivers export approximately 441 kg Hg and 14.6 kg MeHg to the eastern James Bay every year. These rivers account for >94% of the discharge to the eastern James Bay. Assuming that the unsampled rivers export concentrations close to the average, then about 479 Kg Hg and 16.0 kg

MeHg is exported annually along the entire Eastern James Bay, and this number could range from 447 kg to 528 kg Hg and 14.9 kg to 20.0 kg MeHg depending on the concentrations in these unsampled rivers. . Although these estimates of exports are in lower range compared to the export of other major Arctic rivers, primarily due to the smaller watershed area and discharge, Hg export from the whole Eastern James Bay and these Arctic rivers are roughly proportional when considering watershed area (Zolkos et al., 2020). Knowing that the eastern side accounts for around 50% of the area of the whole James Bay watershed, the exports calculated in our study provide an essential estimate to assess overall exports to the bay.

1.8 Conclusions

Our study reinforces current estimates of riverine Hg exports in northern landscapes and the importance of wetlands as sources of MeHg to the aquatic network. However, our results also suggest that landscape features found to be important at local watershed scales may not be entirely transposable to broader regional scales spanning multiple watersheds because large rivers integrate not only the loading of Hg but also the losses accumulating along the entire aquatic network. In particular, we show that the aquatic sink, for which percent water in the catchment is a good proxy in these boreal watersheds in Northern Québec, is the dominant feature driving riverine Hg concentrations, and therefore watershed yields and Hg export to the James Bay. Our results thus improve our fundamental understanding of the broad scale patterns in Hg

cycling, provide scalable relationships based on widely available data on surface water area that can guide future extrapolation efforts and deliver estimates of Hg and MeHg exports and yields for the whole James Bay and other boreal landscapes.

2 CHAPITRE II

HYDROLOGY AND SEASONALITY SHAPE THE COUPLING OF HG AND MEHG WITH DOC IN BOREAL RIVERS OF NORTHERN QUÉBEC

Caroline Fink-Mercier[1], Jean-François Lapierre[2], Marc Amyot[2], Paul del Giorgio[1]

[1] University of Quebec in Montreal, Biology, [2] University of Montreal, Biological sciences

2.1 Acknowledgements

Funding for this project was provided by Niskamoon Corporation, as was part of the Comprehensive Costal Habitat Research Project of Eeyou Istchee, and by master fellowships from the Natural Sciences and Engineering Research Council (NSERC), from the Fond Québécois de la recherche sur la nature et les technologies and from the Ecolac NSERC CREATE training program in Lake and Fluvial Ecology. We would like to thank Niskamoon Corporation members, Cree land users and del Giorgio's lab members for their help during field campaigns and logistics, and Dominic Bélanger for his assistance during laboratory analyses.

2.2 Abstract

Coloading of Hg with DOC is a key driver of the observed spatial and temporal Hg heterogeneity among aquatic ecosystems. Their strong geochemical coupling has therefore spurred the use of DOC as a predictor of Hg concentrations and exports in northern regions where sampling logistics for Hg are costly and complex. Yet relationship between Hg and MeHg with DOC have recently been shown to be highly variable, suggesting that other mechanisms diverging from common loading might be of central importance in driving the relationship between Hg and DOC across landscapes. In this study, we explore the relationship between Hg and MeHg with DOC across 18 major boreal rivers draining the Eastern James Bay (Québec) collectively draining over 350 000 km^2, capturing watersheds with a wide range of vegetation, water residence time and riverine DOC amounts and compositions. Our results show that even though a large portion of the variation in Hg and MeHg are explained by DOC, Hg-DOC and MeHg-DOC relationships and ratios vary greatly both spatially and temporally. We argue that ratios and strength of the coupling could be predicted based on hydrology of the system as suggested by the decline in Hg : DOC and increase in MeHg : DOC ratios and coupling as the seasons progress to warmer seasons, higher water evaporation, and presumably longer retention time. Our study highlights the role of seasonal hydrology and biological processing in governing Hg, MeHg and DOC patterns in northern rivers.

2.3 Introduction

Mercury (Hg) is a globally distributed environmental pollutant with potential neurological effects on wildlife and human health (UN Environment, 2019). When emitted to the atmosphere, it can travel long distances before it deposits on vegetation, soils or aquatic systems, which makes it a contaminant of interest even in remote regions far from anthropogenic sources (Fitzgerald et al., 1998; UN Environment, 2019). Among other issues, identifying areas of high Hg concentrations is essential to evaluate the risk of dietary Hg contamination, especially in remote northern communities where mercury levels in fish and marine mammals are commonly elevated (Gandhi et al., 2014; Lockhart et al., 2005). In these northern regions, adjacent areas may exhibit large variations in watershed Hg yields and riverine Hg concentrations, independently of atmospheric deposition (see Chapter 1, Eklof et al. 2012, Domagalski et al. 2016), and therefore varying Hg export to the ocean (Domagalski et al., 2016). This has spurred significant research on the mechanisms of Hg loading to aquatic systems and the search for drivers explaining the observed spatial and temporal Hg heterogeneity among aquatic ecosystems (Burns et al., 2013; Schelker et al., 2011; Vermilyea et al., 2017; Vidon et al., 2014). Many of these studies have focused on hotspots (Selvendiran et al., 2009; Shanley et al., 2005; St. Louis et al., 1996) and hot moments of Hg delivery to aquatic systems (Kirk & St. Louis, 2008; Schelker et al., 2011; Shanley et al., 2008), such as loading from wetlands and with

spring thaw. The common denominator from these studies is the importance of aquatic organic matter as a predictor.

Co-transport with dissolved organic carbon (DOC) is a key driver of Hg spatial and temporal patterns in aquatic systems (Schelker et al., 2011). The strong affinity of Hg for the aromatic and colored fraction of DOC facilitates the delivery of Hg from soils to streams together with DOC during hydrological events (Burns et al., 2012a; Ravichandran, 2004). This strong geochemical coupling was shown to be expressed by a relatively constant ratio of around 0.2 ng Hg per mg of DOC, which was initially reported in several northern hemisphere studies (Grigal, 2002). This in turn led several studies to suggest the use of DOC (Dittman et al., 2009), or proxies of DOC aromaticity such as fluorescent DOM (Lescord et al., 2018; Vermilyea et al., 2017) and UV absorption (Burns et al., 2013), as potential predictors of Hg concentrations in fluvial networks. This approach would be particularly promising for remote northern regions where sampling logistics for Hg are costly and complex and where Hg remains a public health issue in communities who rely on hunting and fishing. The assumption that the stoichiometry of Hg and DOC co-transport is relatively constant, however, has been challenged by a recent meta-analysis (Lavoie et al., 2019), who reported highly variable slopes of the relationship between Hg and DOC in northern regions across the globe (ranging from 0.003 to 0.91 ng Hg / mg DOC) and also variable strength of the correlation between the two (R^2= -0.34 – 0.99), rendering the prediction of Hg concentrations on the basis of DOC highly uncertain. Although the strength of the

correlation generally improves with aromatic DOC pools compared to bulk DOC, it is also variable across studies and seasons (Burns et al., 2013; Lavoie et al., 2019). This suggests that co-transport of Hg and DOC is not the only mechanism responsible for the coupling of these elements across watersheds, and that other factors are at play in the surrounding catchment or in the fluvial network.

In addition to the co-mobilization of Hg with DOC from soils, processing and losses also shape Hg and DOC concentrations and speciation in aquatic ecosystems. There is evidence of increased decoupling of fluvial Hg and DOC in watersheds with abundant standing waters (Schelker et al., 2011). More specifically, a recent study found a decrease in Hg : DOC ratios in lakes with longer water residence times (Richardson et al., 2020), suggesting that these may represent a preferential sink for Hg vs DOC via relatively higher sedimentation and photodegradation rates. Along the same line, processes that lead to the production of DOC *in situ* but that are not linked to the loading of material from land would tend to decouple Hg from DOC, which may explain the stronger relationships observed between Hg and colored dissolved organic matter compared to relationships between Hg and DOC (Lavoie et al., 2019). Similarly, MeHg concentrations tend to follow DOC patterns when both originate from the catchment (Bravo et al., 2017) whereas elevated levels autochthonous DOC in the aquatic environment have previously been associated to MeHg production (Bravo et al., 2017) and may result in coupling of MeHg concentrations with autochthonous DOC but varying coupling of MeHg with bulk DOC. This coupling between MeHg and

DOC, just as that of Hg with DOC, deserves attention because MeHg : DOC may act an indicator of aquatic ecosystem sensitivity to Hg contamination, with higher potential of accumulation in biota at high ratios (Chételat et al., 2018). The ratios between MeHg and DOC are however also highly variable (Lavoie et al., 2019), which complicates the identification of hotspots or hot moments of MeHg bioaccumulation. Overall, evidence suggests that both Hg and MeHg tend to move together with DOC from land to water, but that conditions associated with increased biogeochemical processing of either DOC or Hg lead to their decreased coupling.

Seasonal and geographic properties that dictate light, temperature and water retention time in rivers should alter the patterns in Hg and DOC processing, with impacts on their coupling. For example, geographic features linked to increased retention time, such as high lake density (Gibson et al., 2015), could be linked to enhanced processing along the aquatic continuum and therefore reduced coupling of Hg with DOC. Similarly, higher discharge during snowmelt in northern regions favor hydrological transport and potentially stronger Hg-DOC coupling compared to base flow conditions favoring retention, transformation and loss of material in aquatic systems (Covino, 2017). Different degrees of coupling between seasons could explain why Lavoie *et al.* (2019) noted important variation in the coupling in temporal studies, yet few investigations have directly addressed the influence of hydrology and seasonal variations on the nature and strength of the Hg-DOC and MeHg-DOC relationships, in part due to the difficulty in obtaining suitable seasonal data in northern environments.

Estimating the relative contribution of transport and processing of Hg and DOC could be done using of water stable isotopes (^{18}O, ^{2}H), an indicator of water processing expressed as the extent of evaporation since precipitation and reflected in the commonly used deuterium excess index. More specifically, enrichment in ^{18}O (higher d-excess values) is generally observed in headwaters and tends to decline towards the mouth, and from spring freshet to summer, as a result of increased evaporation (Gibson et al., 2005). Assuming that the conditions responsible for water evaporation (light, temperature) are at least partly linked to source (Duvert et al., 2020) and biogeochemical processing of Hg (Shanley et al., 2005) and C (Vachon et al., 2016) in the water, seasonal patterns in hydrology should be related to seasonal patterns in Hg vs DOC coupling. However, to our knowledge, only one study has used d-excess to link Hg : DOC and MeHg : DOC ratios to variations in water residence time in lakes and therefore to processing (Richardson et al., 2020), and none to our knowledge has attempted to link patterns in Hg-DOC and MeHg-DOC coupling in rivers to seasonal variations in both discharge and processing of the water in rivers.

Understanding the relationship between Hg and DOC across northern aquatic networks requires on the one hand capturing the environmental heterogeneity that drives their respective watershed balances across the landscape, and also capturing the seasonal variability that is determined by the underlying hydrologic and climatic drivers. In this study, we explore the relationship between Hg and MeHg with DOC across 18 boreal rivers draining into the Eastern James Bay in northern Québec,

spanning a 650 km latitudinal transect and collectively draining over 350 000 km^2, comprising watersheds with a wide range of vegetation, geology, riverine DOC amounts and composition as well as differing in the extent of water coverage and residence time within the watershed. The study was carried over 4 different seasons in order to capture distinct climatic and hydrologic periods, which coupled to the use of stable water isotopes allows us to explore the seasonality of the Hg-DOC and MeHg-DOC dynamics and the relative importance of passive hydrological transport versus processing in shaping these dynamics.

2.4 Methods

2.4.1 Study site description

In this study, a total of 18 rivers were targeted based on their hydrological importance and on right to access and sample in traplines granted by individual tallymen as most of these rivers sampled are situated within the Cree Nation (Eeyou Istchee) territory. Field operations were carried out with full consent from local land users, in collaboration with local communities and with the engagement of Niskamoon Corporation as the framework of this research is embodied in a broader interdisciplinary study investigating the changes in the Coastal habitat of Eeyou Istchee. Rivers range from Strahler order 3 to 9 and are distributed on a 650 km latitudinal transect on the eastern shore of James Bay in the Canadian shield, starting from a

headwater-near lake of Harricana river in Amos, Qc (48,57º N, 78,12º W) in the south to the northernmost site on Salmon river, near the James Bay – Hudson Bay junction (54,63º N, 79,58º W) (Chapter 1, Figure 1.1). This latitudinal transect results in a gradient in temperature, tree cover, soil type, abundance of wetlands. Glacial erosion shaped the low relief and flat top summits of the regions creating an abundance of lakes, ponds and swaps (Natural Resources Canada, 2019). Isolated patches of permafrost cover the region and sporadic discontinuous permafrost is found in the 2 northermost river watersheds (Au Phoque and Salmon rivers) (Natural Ressources Canada, 1995). Hydrology of the region is impacted by extensive hydroelectric development. The Rupert, Eastmain, Sakami, Opinaka, Grande Baleine and Caniapiscau rivers have all been diverted to La Grande watershed which ultimately doubled its natural river discharge (Déry et al., 2016; Messier et al., 1986). Both the abundant lake cover and the river diversions result in watersheds with very different hydrologic patterns, discharges and water residence times.

For each of the 18 rivers, a sampling site at the mouth was determined and, when possible, a site upstream, closest to the headwaters based on access constraints. When the distance between these two sampling sites was higher than 100 km, a sampling site in the middle was determined. These sites were visited a total of 5 times through summer 2018, fall 2018, winter 2019, spring 2019 and summer 2019 (Figure S3), spanning a wide range of hydrological conditions.

2.4.2 Sample collection

Sample collection by boat with Cree guides was prioritized as this project was carried out in collaboration with local communities. However, a majority of samples were collected by helicopter either hovering or landing due to the remote location of the sites. Most rivers were over 1.5 meter depth and hovering was done at a minimum of 2 meter above water, resulting in turbulence limited to surface water, therefore avoiding the resuspension of sediments. When hovering, contact between the helicopter and the samples was limited by pumping water with in a Teflon tube dropped in the water 0.5 meter below surface. For mercury samples, samples were taken in borosilicate glass bottles priorly washed with 50% acid solution (HNO_3 45%, HCl 5%) with a clean sampling protocol adapted for 1 person (Lewis & Brigham, 2004). The samples were collected with a peristaltic pump and half of them were filtered in the field with a reusable 0.45 µm polycarbonate in-line filter. All pumping and filtering material was cleaned with HCl 10% and Nanopure water between sites and rinsed with in situ water before sample collection. Duplicates of field blanks were performed during each sampling campaign using Nanupure water running through the Teflon tube and the filtration system. Mean values of blanks for the 5 campaigns were 0.04 ng L^{-1} of MeHg and 0.06 ng L^{-1} of total Hg, well below ambient concentrations and close to detection limits. All samples were acidified with ultrapure 100% HCl to reach a concentration of 2% in the samples and a pH under 2. Samples were preserved at 4°C

in the dark. Dissolved organic carbon and color (i.e. colored dissolved organic matter, CDOM) samples were taken in HPDE bottles with a peristaltic pump, filtered with 0.45 µm polyethersulfone syringe filter in the lab within hours and stored at 4°C in the dark. Samples for stable water isotopes were collected in 20 mL Nalgene vials ensuring there was no air headspace.

2.4.3 Chemical measurements

Analyses of total mercury were conducted using the Tekran 2600 (Tekran® Instruments Corporation) cold vapor atomic fluorescence spectrometer (CVAFS) with a detection limit of 0.05 ng L^{-1} of Hg and following the 1631 method of the United State Environment Protection Agency (EPA) (U.S. Environmental Protection Agency, 2002). Bromine monochloride, and stannous chloride ($SnCl_2$) were added to samples for oxidation of all Hg form into Hg(II) and conversion of Hg(II) to volatile Hg(0) for further detection onto the cell of a cold-vapor atomic fluorescence spectrometer (CVAFS). Analysis of MeHg was conducted using the Tekran 2700 instrument CVAFS with a detection limit of 0.01 ng L^{-1} and following the 1630 method of the EPA (U.S. Environmental Protection Agency, 2001). Samples were first distilled to remove any interference from organic matter and sulfide residues and pH was adjusted to 4.9 with acetate buffer. Sodium tetraethyl borate ($NaBEt_4$) was added to form methylethyl mercury. In the Tekran 2600, methylethyl mercury was separated from solution with N_2, trapped onto a graphitic carbon trap, carried by argon gas, converted

to elemental mercury (Hg0) and detected into the cell of a CVAFS. Instrument performance and stability were measured with blanks and standards. All mercury analyses were performed on duplicates of filtered samples and duplicates of non-filtered samples. Analyses were discarded and repeated when chemical standards had a standard error above 10% or when samples had a relative standard deviation over 20%. If relative standard deviation was still over 20% within duplicates after repeated measurement, samples were further examined for possible exclusion from the data set. Analytical samples in this study had a mean relative standard deviation of 3.8% for dissolved Hg (n=156 duplicates), 8.0% for dissolved MeHg (n=157 duplicates).

Dissolved organic carbon was measured on a TIC-TOC Analyzer using wet persulfate oxidation (Aurora, College Station, TX, USA). Color was analysed on a Biochrom Ultrospec 3100 Pro spectrophotometer at 440 nm. These samples were blanked using the absorption of nanopure water (Thermo Fisher Scientific Inc., Waltham, MA, USA).

Stable water isotopes, δ18O and δ2H, were measured using a LGR (Los Gatos Research, San Jose, CA, USA) liquid water isotope analyzer, model T-LWIA-45-EP Off-Axis Integrated Cavity Output Spectroscopy (OA-ICOS) (precision = ±0.1‰ for $\delta^{18}O$, ±1.0 ‰ for $\delta^{2}H$) in the Geotop Laboratory, University of Quebec in Montreal. For each sample, there were 10, 1-µL injections, and the first 2 injections of each

sample were rejected to limit memory effects. Raw values were corrected using 3 reference standards on a VSMOW-SLAP scales ($\delta^{18}O$= 0,23±0.06‰, -13,74±0.07‰ and -20,35±0.10‰; $\delta^{2}H$= 1,28±0.27‰, -98,89±1,12‰ and -155,66±0.69‰; $\delta^{17}O$= 0,03±0.04‰, -7,32±0.06‰ and -10,80±0.06‰). A 4th reference water ($\delta^{18}O$= -4,31±0.08‰; $\delta^{2}H$= -25,19±0.83‰; $\delta^{17}O$= -2.31±0.04‰) was analyzed as an unknown to assess the exactness of the normalization. Deuterium excess (d-excess) was calculated as: d-excess= δ2H − 8 * δ18O (Turner et al., 2014).

2.4.4 Statistical analyses

Bivariate regressions between Hg, MeHg and DOC for each season were performed in R 4.0.2 (R Core Team, 2019). Slopes and R^2 of the models are summarized in table 2.1. An ancova followed by a Tukey post-hoc test were performed to detect differences in slopes and results are shown in figure S4. In order to explore the effect of hydrology on the patterns in DOC / Hg coupling within river sites over time, and to isolate these from other co-varying factors, we chose to calculate the changes in water properties and DOC / Hg concentrations within individual sites over time rather than relating the absolute values of water isotopes to material concentrations. To do this, we calculated the change for all sites between pairs of seasons (i.e. spring and summer) for d-excess (Δ d-excess), Hg : DOC (Δ Hg : DOC), MeHg : DOC (Δ MeHg : DOC) and colored DOC : bulk DOC (Δ color : DOC). A total of 207 pairs of sites were computed comparing 5 seasons between each other from 37

individual sites. Bivariate regressions were then performed between Δ d-excess and Δ Hg : DOC and between Δ d-excess and Δ MeHg : DOC. The Δ color : DOC was regressed against Δ d-excess to further explore how hydrology may influence C dynamics within individual sites over times. A summary of the models is shown in table S3.

2.5 Results

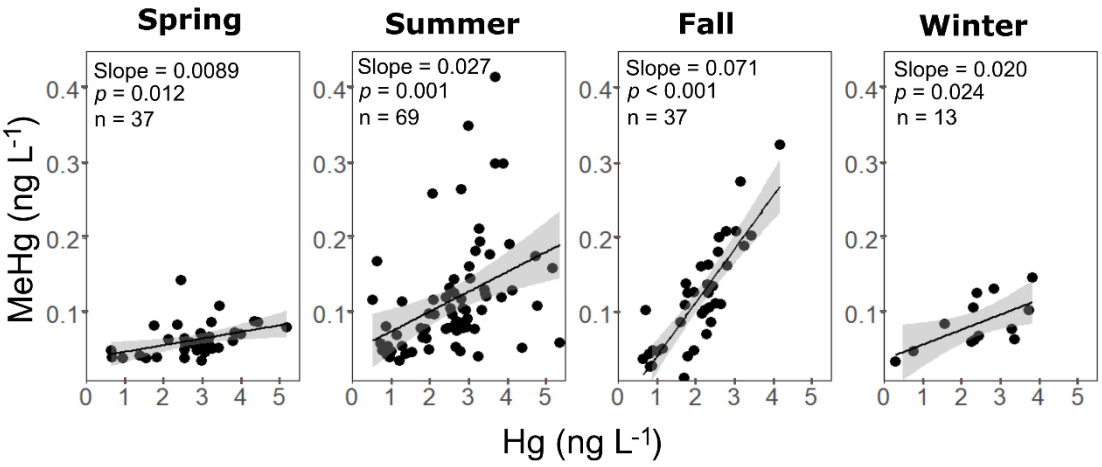

Figure 2.1. Seasonal relationships between Hg and MeHg. Both summer 2018 and 2019 data are shown. Grey areas represent the standard error around the curves.

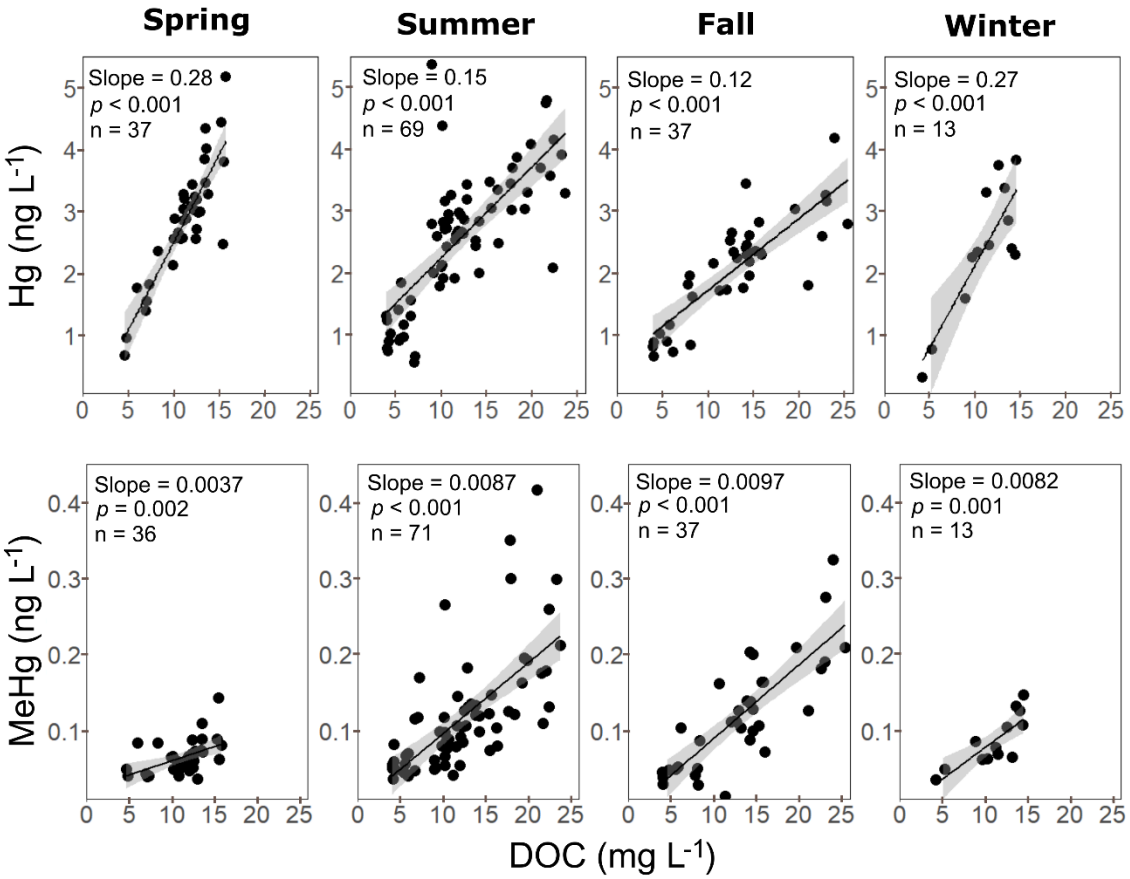

Figure 2.2. Relationship between DOC and Hg (top panels) and MeHg (bottom panels), separated by season. Both summer 2018 and 2019 data are shown. Grey areas represent the standard error around the curves.

Table 2.1. Seasonal slopes and ratios of MeHg-Hg, Hg-DOC and MeHg-DOC relationships. Ratios in bold represent the mean seasonal ratio. Parentheses associated with ratios correspond to the seasonal range in ratios across sites.

		Spring	Summer	Fall	Winter
Slopes	**MeHg-Hg**	**0.0089** (R^2=0.14)	**0.027** (R^2=0.24)	**0.071** (R^2=0.69)	**0.020** (R^2=0.33)
	Hg-DOC	**0.28** (R^2=0.76)	**0.15** (R^2=0.57)	**0.12** (R^2=0.68)	**0.27** (R^2=0.68)
	MeHg-DOC	**0.0037** (R^2=0.22)	**0.0087** (R^2=0.42)	**0.0097** (R^2=0.66)	**0.0082** (R^2=0.62)
Ratios	**%MeHg** (MeHg:Hg)	**2.64** (1.23-7.53)	**5.21** (1.13-25.99)	**5.71** (0.82-14.58)	**4.43** (1.93-11.82)
	Hg:DOC	**0.25** (0.14-0.33)	**0.22** (0.076-0.59)	**0.17** (0.085-0.24)	**0.21** (0.071-0.30)
	MeHg:DOC	**0.0060** (0.0028-0.014)	**0.0098** (0.0038-0.026)	**0.0091** (0.0012-0.017)	**0.0079** (0.0049-0.010)

Riverine concentrations of dissolved Hg and MeHg ranged widely across sites and seasons (Figure 2.1, Table 2.1). Hg concentrations ranged from 0.3 to 5.4 ng L^{-1} and MeHg from 0.01 to 0.42 ng L^{-1}, both forms having the highest concentration during summer. Hg and MeHg were positively correlated, but the strength and the shape of the relationship varied seasonally. The slopes of the relationship between Hg and MeHg (Table 2.1) increased from spring (0.0089) to fall (0.071), together with an increasing mean seasonal ratio of MeHg:Hg (% MeHg). The summer relationship was much more variable with a higher degree of uncoupling between Hg with MeHg and the lowest R^2 (R^2=0.24), contrasting with a stronger coupling during the fall (R^2=0.69). This high degree of variability allowed for some sites to have highest % MeHg during summer even though fall has the highest mean slope and mean overall % MeHg (Figure 2.1, Table 2.1).

The relationships between Hg and DOC varied widely in terms of slopes and strength across seasons (Figure 2.2a, Table 2.1). The coupling between both elements was the strongest in spring, as shown by the highest slope (0.28), mean Hg : DOC ratio (0.25) and correlation strength (R^2=0.76), while fall had the lowest slope (0.12) and summer the lowest correlation coefficient (R^2=0.57). Overall, the Hg : DOC ratio varied 8-fold, ranging from 0.07 to 0.59 ng Hg/mg DOC. The slope of the relationship between MeHg and DOC showed less variation across seasons and weaker overall relationships than for Hg (Figure 2.2b, Table 2.1). Contrary to the pattern observed for

Hg, the weakest coupling between MeHg and DOC was observed in spring, with both the lowest slope (0.0037) and R^2 (0.22), whereas the strongest coupling was observed in the fall (slope = 0.0097, R^2=0.66) (Table 2.1). In fact, the slopes of either MeHg or Hg *vs* DOC followed the exact opposing cross-seasonal pattern, with the slope for MeHg-DOC increasing in the order of spring < winter < summer < fall — an order that also corresponded to increasing proportions of MeHg : Hg—whereas the slope for Hg-DOC had a mirrored order (Table 2.1, Figure 2.2). Mean seasonal ratios of MeHg : DOC and slopes were close between fall and summer, but summer had more variation in ratios evidenced by lower R^2. Overall, MeHg : DOC ratios varied over 20-fold when considering all sites, ranging from 0.0012 to 0.026 ng MeHg/mg DOC. No spatial predictor (e.g. land cover, climate) meaningfully predicted the Hg : DOC or MeHg : DOC ratio.

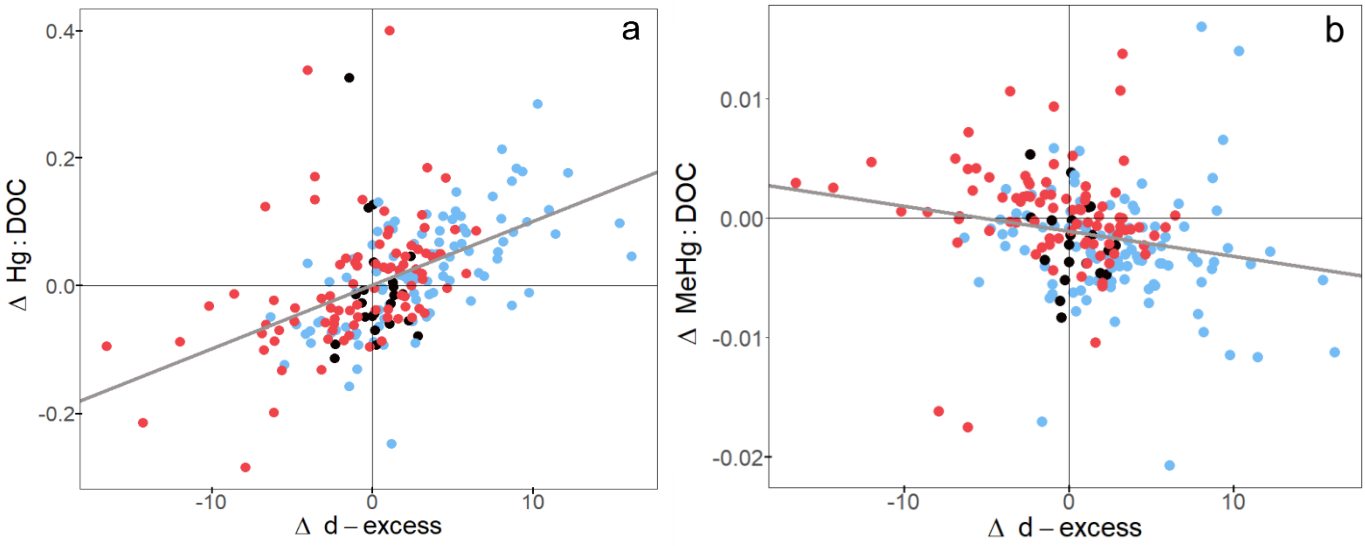

Figure 2.3. Linear relationships between d-excess and seasonal changes in a) Hg:DOC (in ng Hg / mg DOC) and b) MeHg:DOC (in ng MeHg / mg DOC) within individual sites in the 18 rivers sampled. Colored dots represent a change toward a warmer season (red), a colder season (blue) and no change in season (black, e.g. summer 2018 to summer 2019). Each point represents the change between two campaigns carried out in different seasons for any given site. Low d-excess values mean more evaporated water.

The isotopic signature of water in our sites, which we used as an index of water retention time within the network, confirmed that riverine water was more evaporated than in warmer seasons, with generally lower values of d-excess relative to other seasons (Figure 2.3). Overall, changes in Hg : DOC and MeHg : DOC at individual sites were coherent with changes in d-excess across sampling seasons; cross-seasonal change in d-excess was consistently associated with change in these former variables, and the largest cross-seasonal changes in hydrology resulted in the largest changes in Hg : DOC and, to a lesser extent, MeHg : DOC. In particular, the ratios shifted by up to 0.4 ng Hg/mg DOC and 0.02 ng MeHg/mg DOC across pairs of seasons. Moreover,

the opposite direction of these trends suggests a more rapid loss of Hg compared to DOC and, conversely, a gain in MeHg relative to DOC under scenarios of higher evaporation and presumably higher biogeochemical processing within the fluvial network.

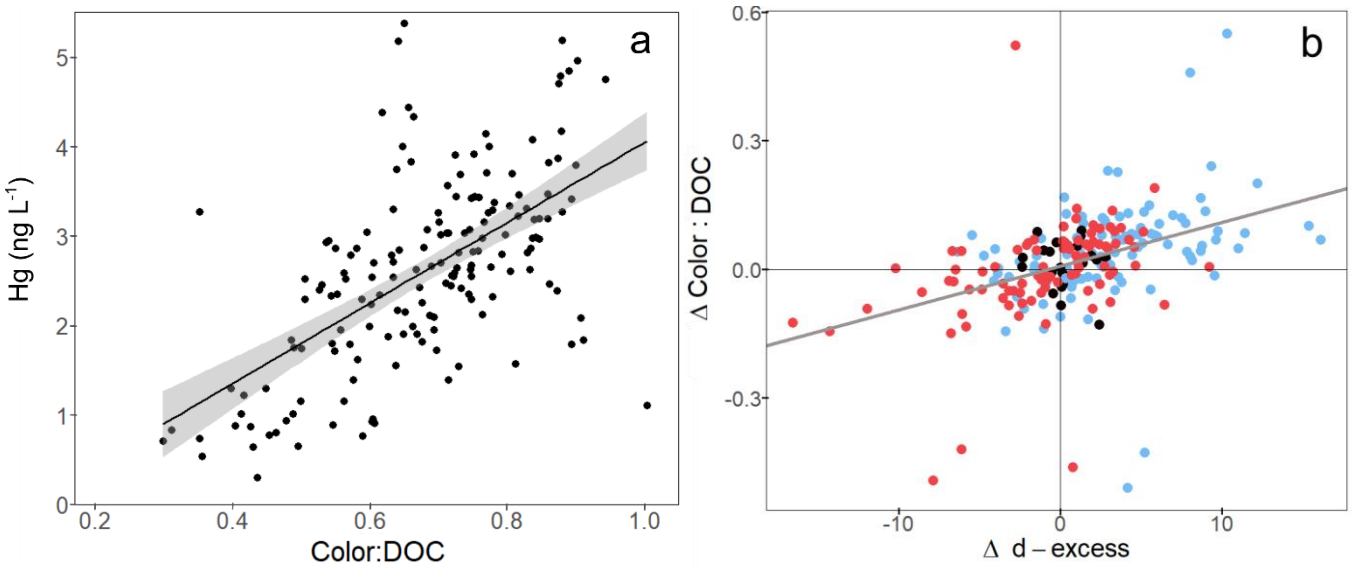

Figure 2.4. Linear relationships between a) the proportion of colored DOC on bulk DOC (in m^{-1} / mg L^{-1}) and Hg and b) between seasonal changes in d-excess and changes in the proportion of colored DOC on bulk DOC (in m^{-1} / mg L^{-1}). Colored dots represent a change toward a warmer season (red), a colder season (blue) and no change in season (black, e.g. summer 2018 to summer 2019). Each point represents the change between two campaigns carried out in different seasons for any given site. The grey area represents the standard error around the curve. Relationships are statistically significant (α= 0.05).

In order to explore the underlying mechanisms linked to the faster loss of Hg relative to DOC, evidenced by the decline in Hg : DOC ratios, with an increase in network-scale evaporation (Figure 2.3), the network patterns of the colored fraction of

DOC (i.e. color) were further investigated. We focused on this fraction of DOC because Hg is generally more tightly coupled to color (Lavoie et al., 2019). This pattern was confirmed for our rivers as per the positive relationship between Hg and the ratio of color : DOC (Figure 2.4a), such that Hg concentrations tend to be higher when a higher proportion of the bulk DOC is comprised by color. There was a pattern of seasonal decline in the ratio of color : DOC as a function of shifts in d-excess, with the largest declines in the proportion of colored DOC occurring in periods with the largest declines in d-excess, suggesting a selective loss of colored DOC relative to bulk DOC in conditions of increased evaporation within the fluvial network.

2.6 Discussion

In this study, we have shown that Hg-DOC and MeHg-DOC relationships and ratios vary greatly both spatially across the 18 boreal rivers, and seasonally within rivers (Figure 2.2, Table 2.1). Specifically, the measured Hg : DOC and MeHg : DOC ratios (Table 2.1) covered much of the range of what has been reported for the Northern hemisphere [0.018-0.22 ng MeHg/mg DOC, (Lavoie et al., 2019)], North America [0.12-1.4 ng Hg/mg DOC, (Stoken et al., 2016)] and Northern streams and rivers [0.001-0.02 ng MeHg/mg DOC, 0.19-2.25 ng Hg/mg DOC (Nagorski et al., 2014; Schuster et al., 2011)]. Ratios within given sites varied by as much as 0.4 ng Hg/mg DOC across seasons (Figure 2.3), which is comparable to the range across all sites. Therefore, for these northern rivers, there was as much variation

within a site over a year than among different sites distributed over a 650 km latitudinal transect at any given moment. Previous studies have explained spatial differences in Hg-C coupling with patterns in Hg deposition on land induced by heterogeneous vegetation patterns (Graydon et al., 2008; Riscassi & Scanlon, 2011) or wetland influence (Burns et al., 2012a) due to local nutrient concentrations, pH and redox conditions that could affect methylation rates in the water or in soils (Tjerngren et al., 2012; Ullrich et al., 2001). We similarly explored potential relationships between the Hg:DOC and MeHg:DOC ratios with land cover and *in situ* nutrient concentrations, but no significant patterns were found. We rather found that at this scale, the ratios and strength of the coupling between Hg, MeHg and DOC were best predicted by seasonal hydrology, and that Hg and MeHg followed opposite patterns in terms of their relationships with DOC. In particular, any increase in DOC led to the highest increase in Hg in moments of high discharge (Table 2.1), likely because they move together from soils to water and there is little opportunity for differential processing due to lower residence times. In contrast, it is at moments of low discharge, higher retention time and during (or following) warm seasons that DOC and MeHg are most tightly coupled and that any increase in DOC leads to the highest increase in MeHg (Table 2.1), hence during seasons with higher potential for cumulative biogeochemical processing of both elements. These same conditions were associated to the highest proportions of MeHg relative to total Hg.

Several mechanisms have been suggested to explain the variable relationships between Hg and DOC, including Hg supply limitation (Stoken et al., 2016), and differential links to hydrological or biogeochemical processing (Schelker et al., 2011). Regarding the latter, a decline in Hg : DOC ratios has been reported in lakes of longer water residence time (Richardson et al., 2020), and increased decoupling has been reported during the growing season relative to spring snowmelt (Schelker et al., 2011), presumably due to unequal photochemical and biological processing of Hg relative to DOC. We observed a similar pattern that was related to declines in d-excess, which potentially reflects increased evaporation and therefore longer water residence time within the network (Figure 2.3). These patterns suggest that the weakening Hg-DOC coupling and the decline in ratios from spring to fall in our studied rivers may reflect increased processing during the summer and unequal within-network losses of Hg and DOC when water residence time increases, which could explain why weaker relationships have typically been reported in studies that included a seasonal dimension (Lavoie et al., 2019). These results highlight the role of hydrology as a key driver of Hg-DOC coupling, favoring co-transport and tight coupling under high flushing conditions, and preferential loss of Hg over DOC and weaker coupling under scenarios of longer network residence time combined with conditions that favor processing.

The underlying mechanism responsible for the selective loss of Hg relative to bulk DOC with increased evaporation could reside in the preferential association

between Hg and the colored fraction of DOC, the latter being mostly of terrestrial origin (Creed et al., 2018; Ravichandran, 2004). Numerous studies have found a stronger relationship between Hg and the aromatic and colored dissolved organic matter pools due to strong binding of Hg at their reduced sulfur sites, which initially motivated the use of SUVA, FDOM or UV254 as proxies of aqueous Hg (Burns et al., 2013; Dittman et al., 2010; Riscassi & Scanlon, 2011). Likewise, we showed an increase in Hg as DOC becomes more colored in these boreal rivers (Figure 2.4a). Across seasons, DOC becomes depleted in its colored fraction as evaporation increases (Figure 2.4b) and, at the same time, Hg decreases relative to DOC (Figure 2.3). This concomitant decrease in color : DOC and Hg : DOC ratios with increase in evaporation, and therefore longer water residence time, suggests at least two hypotheses. First, increased evaporation in summer could be indirectly linked to conditions of enhanced proportion of autochthonous DOC within the network (Hosen et al., 2020), i.e. a source of DOC that is not associated to the co-loading of Hg with DOC from land or for which Hg has less affinity due to fewer strong sulfur binding sites compared to colored terrestrial DOC (Lescord et al., 2018). However, although enhanced autochthonous inputs could explain the weakening relationship during summer, it is less likely to explain the decline in the ratio of Hg : DOC when water retention increases (as indicated by decreased d-excess, Figure 2.3) because a similar decline in Hg : DOC has been previously linked to water residence time in lakes independently of differences in productivity (Richardson et al., 2020). Instead, we argue that the decline in the ratio of

Hg : DOC is related to the preferential loss of both Hg and colored DOC over bulk DOC. Colored DOC has been shown to be preferentially lost during transit in the aquatic network, because it is particularly susceptible to photo-oxidation or flocculation and there is little production of colored DOC in lakes and rivers, while autochthonous, non-colored DOC is constantly replenished along the aquatic continuum (Hutchins et al., 2017; Kothawala et al., 2014; Weyhenmeyer et al., 2012). Consequently, Hg and colored DOC could either sediment and be buried together, as demonstrated by the strong relationship between SUVA (Jiang et al., 2018) or cDOM (Isidorova et al., 2016) and Hg concentration in sediments, or be otherwise processed and removed at similar rates through photo-oxidation, resulting in a remaining DOC pool that is not as closely associated to Hg as the DOC that was loaded from land. Therefore, we not only found a close association between Hg and terrestrially derived DOC due to their common loading as it has been shown before (Burns et al., 2013; Lescord et al., 2018), but our results further suggest that Hg and colored DOC of terrestrial origin are also linked because they are lost at comparable rates at the network level, leaving behind a DOC pool that is less colored and with a lower Hg : DOC ratio.

Although several studies reported a certain degree of coupling between MeHg and DOC, this relationship is usually weaker than with total Hg (Burns et al., 2012b; Lavoie et al., 2019; Lescord et al., 2018) as we have also shown here for boreal rivers. MeHg and DOC have been shown to be coupled when produced at the same place

(Bravo et al., 2017). This can happen, for example, when MeHg is produced in the catchment and exported downstream together with terrigenous DOC (Bravo et al., 2017). In our study we found the highest correlation strength during the fall, most likely reflecting MeHg production in wetlands and riparian anaerobic soils during the growing season followed by the hydrological reconnection of these sources of both MeHg and DOC with the main network during fall discharge events (Branfireun et al., 1996; Selvendiran et al., 2008b). This is consistent with the finding that a large portion of MeHg produced in wetlands, which are abundant in our study area, accumulates and is mobilized to streams during storms, which are more frequent during fall (Branfireun et al., 1996). In contrast, the MeHg-DOC coupling was weak during spring and the ratios were low, likely because of the colder temperature and shorter water residence time during the spring freshet that are unfavorable for MeHg production and accumulation along the aquatic continuum. In such conditions, DOC exports from land to water are still high (Lung et al., 2018), but Hg exports are mostly under the inorganic form given the low rates of methylation (Driscoll et al., 1998). Although spring has recently been shown to be the period of peak MeHg concentrations in some Northern lakes and reservoirs, possibly due to both winter anoxia and absence of photodegradation under ice cover (De Bonville et al., 2020; Varty et al., 2020) , this pattern was not present in our large rivers (Table 2.1, Figure 2.1), potentially due to rapid photodegradation following spring thaw. The intermediate coupling found during summer can be explained by the increased MeHg production, as shown by higher %

MeHg (Table 2.1), where production of MeHg is not necessarily accompanied by equivalent DOC inputs, because MeHg production depends on specific environmental conditions (Gilmour et al., 2013) that may not be associated to enhanced DOC processing. Contrary to the patterns we showed with Hg, which were likely explained by the co-transport and a strong biogeochemical link to the colored DOC pool, the relationship between MeHg and DOC appears to be driven mostly by the seasonal and spatial patterns of production of MeHg. It is interesting to note that Richardson et al. (2020) reported a trend of lower MeHg : DOC ratios in lakes of longer water residence time, which they attributed to higher MeHg photodegradation rates compared to DOC. This would suggest that water residence time may play different roles in modulating the MeHg-DOC coupling depending on the type of ecosystem and the environmental and temporal context. The patterns we observed in these boreal rivers appear to be driven by large seasonal differences in MeHg production, confirming the importance of seasonality on the loading and production of MeHg in aquatic systems (Hill et al., 2009; Selvendiran et al., 2008a; Shanley et al., 2005) and therefore on MeHg and DOC relationships; in this context, summer and fall discharge patterns, longer network residence time and the resulting patterns in stable water isotopes are proxies of these environmental conditions that favor methylation. The patterns reported by Richardson et al. (2020) across lakes, on the other hand, do not emphasize seasonality but rather lake trophic status and productivity. In this regard, long lake water residence time may be a proxy for both low overall productivity (and thus environmental conditions that

do not favor methylation), also for greater potential for MeHg removal. It is therefore important to differentiate the seasonal from the ecosystem components related to differences in water residence time and degradation rates, particularly when transposing spatial results to temporal studies and vice versa. Regardless, our results show that DOC and MeHg are neither as coupled nor as well related to changes in hydrology as DOC and Hg are.

Based on temporally varying Hg : DOC and MeHg : DOC ratios, we estimated the potential bias in calculation of the export of both forms of Hg from these northern rivers using DOC as a proxy. Estimation of Hg and MeHg concentrations from DOC was highly variable (0.03-0.22 ng MeHg and 0.85-5.64 ng Hg), and the modelled export, expressed in kg y^{-1}, diverged from true exports (see Chapter 1) by 22% and 19% on average for MeHg and Hg respectively. This highlights that the use of an average Hg : DOC and MeHg : DOC ratio to model exports might lead to potentially significant biases in specific rivers. However, taken at the regional level, the DOC-based export calculation results in an underestimation of only 2% of MeHg and 10% of Hg exports when summing up exports from all sampled sites. Our results thus suggest that DOC may not be an effective proxy of Hg or MeHg concentration at the individual river scale over time, but may indeed be a robust proxy of Hg and MeHg exports at the regional scale where other sources of variation, particularly temporal, are attenuated. In conclusion, our results show that a large portion of the variation in Hg and MeHg are

explained by DOC across these 18 rivers that span a 650 km gradient of boreal biome, yet Hg : DOC and MeHg : DOC ratios are highly variable across sites and seasons. Our results highlight the importance of seasonal hydrology to the coupling of Hg and DOC through co-transport along the aquatic continuum and the importance of biogeochemical processing to the coupling of DOC and MeHg at warm and low discharge scenarios, with implications for our understanding of the coupling of the Hg and C cycles.

CONCLUSION

Les résultats de mon projet de maîtrise ont permis de mieux comprendre les mécanismes dominants d'apports et de pertes de Hg dans les grandes rivières nordiques de l'Est de la Baie James. Plus précisément, les résultats du premier chapitre de ma maîtrise démontrent que les éléments du paysage importants à échelle locale agissant comme sources ou puits ne sont pas entièrement transposables à une échelle plus large puisque les grandes rivières intègrent non seulement les sources, mais également les puits de Hg et MeHg le long du continuum aquatique. Bien que nos résultats confirment l'importance des milieux humides comme source de MeHg, tel qu'abondamment démontré dans les études dans de petites rivières, ils indiquent que la proportion du bassin versant recouverte d'eau, un proxy des pertes de Hg dans les milieux aquatiques, est l'élément dominant influençant les concentrations de Hg et MeHg dans nos 18 grandes rivières de la Baie James couvrant un territoire de plus de 350 000 km^2. Une plus grande proportion de milieux aquatiques dans les bassins versants accroit les pertes en Hg, d'autant plus durant les saisons de bas débit, diminuant les concentrations et se répercutant ainsi sur les exports et les flux vers la Baie James. Notre étude améliore donc nos connaissances fondamentales sur les patrons de Hg à grande échelle ainsi qu'à l'échelle de rivières individuelles et fournit des relations transposables à

d'autres systèmes, entre le paysage et les concentrations, basées sur des données géographiques facilement accessibles afin de guider les futurs efforts d'extrapolation. Elle propose également des estimations des exports et des flux pour tout le bassin versant de la Baie James évaluées à to 441 kg Hg et 14.6 kg MeHg annuellement, avec des flux moyens par unité de surface de bassin versant de 1.70 g Hg km^{-2} an^{-1} et 0.060 g MeHg km^{-2} an^{-1}. Ces estimés raffineront les budgets pan-canadiens et panarctiques, puisqu'on ignorait jusqu'à maintenant les flux de cette région nordique couvrant près du tiers du paysage Québécois. Localement, les modèles ainsi que les mesures de concentrations et de flux de Hg et MeHg présentés sont particulièrement intéressants pour les communautés de l'Est de la Baie James, qui ont été impactées par l'augmentation des concentrations en Hg dans les milieux aquatiques suite à la création du complexe hydroélectrique de La Grande et qui restent préoccupées par l'intoxication chronique au mercure.

Ayant démontré l'importance de certains éléments du paysage à grande échelle en comparant différents bassins versants et leurs concentrations, le 2^{e} chapitre de ma maîtrise se concentre plutôt sur les variations dans les relations Hg et MeHg avec le COD. Nos résultats démontrent que, bien que le COD explique une grande part de la variation dans les concentrations de Hg et MeHg, les relations Hg-COD et MeHg-COD ainsi que les ratios sont hautement variables, avec presque autant de variation entre les sites qu'entre les saisons pour un site donné. Nos résultats démontrent notamment que ces variations sont grandement modulées par l'hydrologie, suggérant qu'un temps de

rétention plus long se répercute par des pertes différentielles en Hg et COD et mène à un plus faible couplage et de plus petit ratios Hg : COD. Nous argumentons que des pertes plus rapides de Hg comparativement au COD sont probablement dues à de plus hauts taux de photodégradation et de sédimentation en tandem avec la portion colorée du COD, pour laquelle le Hg a davantage d'affinité chimique. À l'opposé, un plus fort couplage MeHg-COD et de plus grands ratios sont observés durant les moments de haut temps de rétention d'eau pendant (et suivant) la saison estivale. Nous argumentons que ces patrons sont dus à l'accumulation de MeHg dans les milieux humides et les zones ripariennes pendant l'été - qui sont également des sources de COD – qui est ensuite co-transporté avec le COD durant les crues automnales. En exposant la haute variabilité saisonnière des relations entre le COD et les formes de Hg, notre étude amène un nouveau regard sur les mécanismes d'apports et de pertes du Hg en tandem avec le COD dans les écosystèmes aquatiques, souligne l'importance de l'hydrologie sur leur couplage et remet en question l'utilisation du COD comme indicateur de Hg dans les rivières éloignées.

Ensemble, nos 2 études démontrent que le paysage et le transport avec le COD exercent un fort contrôle sur les concentrations et exports de Hg dans les grandes rivières nordiques résultant en des relations robustes entre le paysage et les concentrations en Hg ainsi qu'entre le COD. Elles soulignent toutefois l'importance de la saisonnalité et de ses conséquences hydrologiques sur ces relations se répercutant sur le destin du Hg. Suite à ces résultats, il serait intéressant d'évaluer s'il est possible

d'appliquer ces tendances à d'autres grandes rivières nordiques, notamment afin de consolider l'utilisation de la couverture en eau comme indicateur des concentrations aquatiques en Hg dans les grandes rivières nordiques. Considérant l'importance de l'hydrologie sur les sources et les puits de Hg, de prochaines études devraient également se pencher sur l'impact l'intensification des régimes hydrologiques, attendus avec les changements climatiques, sur les apports, les pertes et les transformations de Hg par certains éléments du paysage et en tandem avec le COD. Nos résultats, ainsi que ces pistes de recherches, pourront ainsi aider à d'identifier les rivières de régions éloignées susceptibles d'avoir des concentrations élevées en mercure et à risques de voir leurs flux et exports de Hg augmenter dans le futur.

RÉFÉRENCES

Agriculture and Agri-Foods Canada. (2015). *ISO 19131 – Land Use 1990, 2000, 2010 Data Product Specifications*.

AMAP/UNEP. (2013). AMAP/UNEP Technical Background Report for the Global Mercury Assessment 2013. Arctic Monitoring and Assessment Programme and United Nations Environment Programme, Geneva, Switzerland.

Amos, H. M., Jacob, D. J., Kocman, D., Horowitz, H. M., Zhang, Y., Dutkiewicz, S., et al. (2014). Global biogeochemical implications of mercury discharges from rivers and sediment burial. *Environmental Science & Technology, 48*(16), 9514-9522. https://doi.org/10.1021/es502134t

Amos, H. M., Jacob, D. J., Streets, D. G., & Sunderland, E. M. (2013). Legacy impacts of all-time anthropogenic emissions on the global mercury cycle. *Global Biogeochemical Cycles, 27*(2), 410-421. http://doi.org/10.1002/gbc.20040

Babiarz, C. L., Benoit, J. M., Shafer, M. M., Andren, A. W., Hurley, J. P., & Webb, D. A. (1998). Seasonal influences on partitioning and transport of total and methylmercury in rivers from contrasting watersheds. *Biogeochemistry, 41*(3), 237-257. https://doi.org/10.1023/A:1005940630948

Bates, D. M. (2010). lme4: Mixed-effects modeling with R. In: Springer New York.

Benoit, J. M., Gilmour, C. C., Heyes, A., Mason, R. P., & Miller, C. L. (2002). Chapter 19 : Geochemical and biological controls over methylmercury production and degradation in aquatic ecosystems. *Biogeochemistry of Environmentally Important Trace Elements*, 262-297. http://doi.org/10.1021/bk-2003-0835.ch019

Branfireun, B. A., Heyes, A., & Roulet, N. T. (1996). The hydrology and methylmercury dynamics of a Precambrian Shield headwater peatland. *Water Resources Research, 32*(6), 1785-1794. https://doi.org/10.1029/96WR00790

Braune, B. M., Outridge, P., Fisk, A., Muir, D., Helm, P., Hobbs, K., et al. (2005). Persistent organic pollutants and mercury in marine biota of the Canadian Arctic: An overview of spatial and temporal trends. *Science of the Total Environment, 351*, 4-56. https://doi.org/10.1016/j.scitotenv.2004.10.034

Bravo, A. G., Bouchet, S., Tolu, J., Bjorn, E., Mateos-Rivera, A., & Bertilsson, S. (2017). Molecular composition of organic matter controls methylmercury formation in boreal lakes. *Nature Communications, 8*, 14255. https://www.ncbi.nlm.nih.gov/pubmed/28181492

Bravo, A. G., Kothawala, D. N., Attermeyer, K., Tessier, E., Bodmer, P., Ledesma, J. U., et al. (2018). The interplay between total mercury, methylmercury and

dissolved organic matter in fluvial systems: A latitudinal study across Europe. *Water Research, 144*, 172-182. http://doi.org/10.1016/j.watres.2018.06.064

Brigham, M. E., Wentz, D. A., Aiken, G. R., & Krabbenhoft, D. P. (2009). Mercury Cycling in Stream Ecosystems. 1. Water Column Chemistry and Transport. *Environmental Science & Technology, 43*(8), 2720-2725. <Go to ISI>://WOS:000265172800012

Burns, D. A., Aiken, G. R., Bradley, P. M., Journey, C. A., & Schelker, J. (2013). Specific ultra-violet absorbance as an indicator of mercury sources in an Adirondack River basin. *Biogeochemistry, 113*(1-3), 451-466. http://doi.org/10.1007/s10533-012-9773-5

Burns, D. A., Riva-Murray, K., Bradley, P. M., Aiken, G. R., & Brigham, M. E. (2012a). Landscape controls on total and methyl Hg in the upper Hudson River basin, New York, USA. *Journal of Geophysical Research: Biogeosciences, 117*(G1). https://doi.org/10.1029/2011JG001812

Burns, D. A., Riva‐Murray, K., Bradley, P., Aiken, G., & Brigham, M. (2012b). Landscape controls on total and methyl Hg in the upper Hudson River basin, New York, USA. *Journal of Geophysical Research: Biogeosciences, 117*(G1). https://doi.org/10.1029/2011JG001812

Cariccio, V. L., Samà, A., Bramanti, P., & Mazzon, E. (2019). Mercury involvement in neuronal damage and in neurodegenerative diseases. *Biological trace element research, 187*(2), 341-356. https://doi.org/10.1007/s12011-018-1380-4

Chételat, J., Richardson, M. C., MacMillan, G. A., Amyot, M., & Poulain, A. J. (2018). Ratio of methylmercury to dissolved organic carbon in water explains methylmercury bioaccumulation across a latitudinal gradient from north-temperate to arctic lakes. *Environmental Science & Technology, 52*(1), 79-88. https://doi.org/10.1021/acs.est.7b04180

Covino, T. (2017). Hydrologic connectivity as a framework for understanding biogeochemical flux through watersheds and along fluvial networks. *Geomorphology, 277*, 133-144. https://doi.org/10.1016/j.geomorph.2016.09.030

Creed, I. F., Bergström, A. K., Trick, C. G., Grimm, N. B., Hessen, D. O., Karlsson, J., et al. (2018). Global change‐driven effects on dissolved organic matter composition: Implications for food webs of northern lakes. *Global Change Biology, 24*(8), 3692-3714. https://doi.org/10.1111/gcb.14129

De Bonville, J., Amyot, M., del Giorgio, P., Tremblay, A., Bilodeau, F., Ponton, D. E., & Lapierre, J. F. (2020). Mobilization and transformation of mercury across a dammed boreal river are linked to carbon processing and hydrology. *Water Resources Research, 56*(10), e2020WR027951. https://doi.org/10.1029/2020WR027951

Déry, S. J., Hernandez‐Henriquez, M. A., Burford, J. E., & Wood, E. F. (2009). Observational evidence of an intensifying hydrological cycle in northern Canada. *Geophysical Research Letters, 36*(13). https://doi.org/10.1029/2009GL038852

Déry, S. J., Stadnyk, T. A., MacDonald, M. K., & Gauli-Sharma, B. (2016). Recent trends and variability in river discharge across northern Canada. *Hydrology and Earth System Sciences, 20*(12), 4801-4818. https://doi.org/10.5194/hess-20-4801-2016

DeWitt, P. (2019). ensr: Elastic Net SearcheR. Retrieved from https://cran.r-project.org/web/packages/ensr/index.html

Dittman, J. A., Shanley, J. B., Driscoll, C. T., Aiken, G. R., Chalmers, A. T., & Towse, J. E. (2009). Ultraviolet absorbance as a proxy for total dissolved mercury in streams. *Environmental Pollution, 157*(6), 1953-1956. https://doi.org/10.1016/j.envpol.2009.01.031

Dittman, J. A., Shanley, J. B., Driscoll, C. T., Aiken, G. R., Chalmers, A. T., Towse, J. E., & Selvendiran, P. (2010). Mercury dynamics in relation to dissolved organic carbon concentration and quality during high flow events in three northeastern US streams. *Water Resources Research, 46*. http://doi.org/10.1029/2009wr008351

Domagalski, J., Majewski, M. S., Alpers, C. N., Eckley, C. S., Eagles-Smith, C. A., Schenk, L., & Wherry, S. (2016). Comparison of mercury mass loading in streams to atmospheric deposition in watersheds of Western North America: Evidence for non-atmospheric mercury sources. *Science of the Total Environment, 568*, 638-650. http://doi.org/10.1016/j.scitotenv.2016.02.112

Driscoll, C. T., Holsapple, J., Schofield, C. L., & Munson, R. (1998). The chemistry and transport of mercury in a small wetland in the Adirondack region of New York, USA. *Biogeochemistry, 40*(2-3), 137-146. https://doi.org/10.1023/A:1005989229089

Duvert, C., Hutley, L. B., Birkel, C., Rudge, M., Munksgaard, N. C., Wynn, J. G., et al. (2020). Seasonal shift from biogenic to geogenic fluvial carbon caused by changing water sources in the wet‐dry tropics. *Journal of Geophysical Research: Biogeosciences, 125*(2), e2019JG005384. https://doi.org/10.1029/2019JG005384

Eklof, K., Folster, J., Sonesten, L., & Bishop, K. (2012). Spatial and temporal variation of THg concentrations in run-off water from 19 boreal catchments, 2000-2010. *Environ Pollut, 164*, 102-109. http://doi.org/10.1016/j.envpol.2012.01.024

Engstrom, D. R. (2007). Fish respond when the mercury rises. *Proceedings of the National Academy of Sciences, 104*(42), 16394-16395.

Fisher, J. A., Jacob, D. J., Soerensen, A. L., Amos, H. M., Steffen, A., & Sunderland, E. M. (2012). Riverine source of Arctic Ocean mercury inferred from atmospheric observations. *Nature Geoscience, 5*(7), 499-504. https://doi.org/10.1038/ngeo1478

Fitzgerald, W. F., Engstrom, D. R., Mason, R. P., & Nater, E. A. (1998). The case for atmospheric mercury contamination in remote areas. *Environmental Science & Technology, 32*(1), 1-7. https://doi.org/10.1021/es970284w

Fleck, J. A., Marvin-DiPasquale, M., Eagles-Smith, C. A., Ackerman, J. T., Lutz, M. A., Tate, M., et al. (2016). Mercury and methylmercury in aquatic sediment across western North America. *Science of the Total Environment, 568*, 727-738. http://doi.org/10.1016/j.scitotenv.2016.03.044

Gandhi, N., Tang, R. W., Bhavsar, S. P., & Arhonditsis, G. B. (2014). Fish mercury levels appear to be increasing lately: A report from 40 years of monitoring in the province of Ontario, Canada. *Environmental Science & Technology, 48*(10), 5404-5414. https://doi.org/10.1021/es403651x

Gibson, J., Birks, S., Yi, Y., & Vitt, D. (2015). Runoff to boreal lakes linked to land cover, watershed morphology and permafrost thaw: A 9 ‐ year isotope mass balance assessment. *Hydrological Processes, 29*(18), 3848-3861. https://doi.org/10.1002/hyp.10502

Gibson, J., Edwards, T., Birks, S., St Amour, N., Buhay, W., McEachern, P., et al. (2005). Progress in isotope tracer hydrology in Canada. *Hydrological Processes: An International Journal, 19*(1), 303-327. https://doi.org/10.1002/hyp.5766

Gilmour, C. C., Podar, M., Bullock, A. L., Graham, A. M., Brown, S. D., Somenahally, A. C., et al. (2013). Mercury methylation by novel microorganisms from new environments. *Environmental Science & Technology, 47*(20), 11810-11820.

Girard, C., Leclerc, M., & Amyot, M. (2016). Photodemethylation of methylmercury in eastern Canadian Arctic thaw pond and lake ecosystems. *Environmental Science & Technology, 50*(7), 3511-3520. https://doi.org/10.1021/acs.est.5b04921

Gouvernment of Quebec. (2019). *Géobase du réseau hydrographique du Québec (GRHQ)*. Retrieved from https://www.donneesquebec.ca/recherche/dataset/grhq.

Government of Canada. (2020a). Historical Climatic Data. Retrieved from https://climate.weather.gc.ca/index_e.html

Government of Canada. (2020b). Historical Hydrometric Data Search. Retrieved from https://wateroffice.ec.gc.ca/search/historical_e.html

Graydon, J. A., St. Louis, V. L., Hintelmann, H., Lindberg, S. E., Sandilands, K. A., Rudd, J. W., et al. (2008). Long-term wet and dry deposition of total and methyl mercury in the remote boreal ecoregion of Canada. *Environmental Science & Technology, 42*(22), 8345-8351. https://doi.org/10.1021/es801056j

Graydon, J. A., St. Louis, V. L., Lindberg, S. E., Sandilands, K. A., Rudd, J. W., Kelly, C. A., et al. (2012). The role of terrestrial vegetation in atmospheric Hg deposition: Pools and fluxes of spike and ambient Hg from the METAALICUS experiment. *Global Biogeochemical Cycles, 26*(1). https://doi.org/10.1029/2011GB004031

Grigal, D., Kolka, R. K., Fleck, J., & Nater, E. (2000). Mercury budget of an upland-peatland watershed. *Biogeochemistry, 50*(1), 95-109. https://10.1023/A:1006322705566

Grigal, D. F. (2002). Inputs and outputs of mercury from terrestrial watersheds: A review. *Environmental Reviews, 10*(1), 1-39. https://10.1139/a01-013

Guay, C., Minville, M., & Braun, M. (2015). A global portrait of hydrological changes at the 2050 horizon for the province of Québec. *Canadian Water Resources Journal / Revue canadienne des ressources hydriques, 40*(3), 285-302. https://10.1080/07011784.2015.1043583

Hall, B., Bodaly, R., Fudge, R., Rudd, J., & Rosenberg, D. (1997). Food as the dominant pathway of methylmercury uptake by fish. *Water, Air, and Soil Pollution, 100*(1-2), 13-24. https://doi.org/10.1023/A:1018071406537

Hammerschmidt, C. R., & Fitzgerald, W. F. (2006). Photodecomposition of methylmercury in an arctic Alaskan lake. *Environmental Science & Technology, 40*(4), 1212-1216. https://doi.org/10.1021/es0513234

Hare, A., Stern, G. A., Macdonald, R. W., Kuzyk, Z. Z., & Wang, F. (2008). Contemporary and preindustrial mass budgets of mercury in the Hudson Bay Marine System: The role of sediment recycling. *Science of the Total Environment, 406*(1-2), 190-204. https://doi.org/10.1016/j.scitotenv.2008.07.033

Hill, J. R., O'Driscoll, N. J., & Lean, D. R. (2009). Size distribution of methylmercury associated with particulate and dissolved organic matter in freshwaters. *Science of the Total Environment, 408*(2), 408-414. https://doi.org/10.1016/j.scitotenv.2009.09.030

Hines, N. A., & Brezonik, P. L. (2007). Mercury inputs and outputs at a small lake in northern Minnesota. *Biogeochemistry, 84*(3), 265-284. Article. http://doi.org/10.1007/s10533-007-9114-2

Hosen, J. D., Aho, K. S., Fair, J. H., Kyzivat, E. D., Matt, S., Morrison, J., et al. (2020). Source switching maintains dissolved organic matter chemostasis across discharge levels in a large temperate river network. *Ecosystems*. http://doi.org/10.1007/s10021-020-00514-7

Hutchins, R. H., Aukes, P., Schiff, S. L., Dittmar, T., Prairie, Y. T., & del Giorgio, P. A. (2017). The optical, chemical, and molecular dissolved organic matter succession along a boreal soil - stream - river continuum. *Journal of Geophysical Research: Biogeosciences, 122*(11), 2892-2908. https://doi.org/10.1002/2017JG004094

Isidorova, A., Bravo, A. G., Riise, G., Bouchet, S., Björn, E., & Sobek, S. (2016). The effect of lake browning and respiration mode on the burial and fate of carbon and mercury in the sediment of two boreal lakes. *Journal of Geophysical Research: Biogeosciences, 121*(1), 233-245. http://doi.org/10.1002/2015jg003086

Jiang, T., Bravo, A. G., Skyllberg, U., Bjorn, E., Wang, D. Y., Yan, H. Y., & Green, N. W. (2018). Influence of dissolved organic matter (DOM) characteristics on dissolved mercury (Hg) species composition in sediment porewater of lakes from southwest China. *Water Research, 146*, 146-158. http://doi.org/10.1016/j.watres.2018.08.054

Kirk, J. L., & St. Louis, V. L. (2008). Multiyear total and methyl mercury exports from two major sub-arctic rivers draining into Hudson Bay, Canada. *Environmental Science & Technology, 43*, 2254-2261. https://doi.org/10.1021/es803138z

Kolka, R. K., Grigal, D. F., Verry, E. S., & Nater, E. A. (1999a). Mercury and organic carbon relationships in streams draining forested upland peatland watersheds. *Journal of Environmental Quality, 28*(3), 766-775. https://10.2134/jeq1999.00472425002800030006x

Kolka, R. K., Nater, E., Grigal, D., & Verry, E. (1999b). Atmospheric inputs of mercury and organic carbon into a forested upland/bog watershed. *Water, Air, and Soil Pollution, 113*(1-4), 273-294. https://doi.org/10.1023/A:1005020326683

Kothawala, D. N., Stedmon, C. A., Müller, R. A., Weyhenmeyer, G. A., Köhler, S. J., & Tranvik, L. J. (2014). Controls of dissolved organic matter quality: Evidence from a large‐scale boreal lake survey. *Global Change Biology, 20*(4), 1101-1114. http://doi.org/10.1111/gcb.12488

Larssen, T., de Wit, H. A., Wiker, M., & Halse, K. (2008). Mercury budget of a small forested boreal catchment in southeast Norway. *Science of the Total Environment, 404*(2-3), 290-296. https://doi.org/10.1016/j.scitotenv.2008.03.013

Laudon, H., Berggren, M., Ågren, A., Buffam, I., Bishop, K., Grabs, T., et al. (2011). Patterns and dynamics of dissolved organic carbon (DOC) in boreal streams: The role of processes, connectivity, and scaling. *Ecosystems, 14*(6), 880-893. http://doi.org/10.1007/s10021-011-9452-8

Lavoie, R. A., Amyot, M., & Lapierre, J. F. (2019). Global meta-analysis on the relationship between mercury and dissolved organic carbon in freshwater environments. *Journal of Geophysical Research-Biogeosciences, 124*(6), 1508-1523. Article. http://doi.org/10.1029/2018jg004896

Lepistö, A., Granlund, K., Kortelainen, P., & Räike, A. (2006). Nitrogen in river basins: Sources, retention in the surface waters and peatlands, and fluxes to estuaries in Finland. *Science of the Total Environment, 365*(1-3), 238-259. https://doi.org/10.1016/j.scitotenv.2006.02.053

Lescord, G. L., Emilson, E. J. S., Johnston, T. A., Branfireun, B. A., & Gunn, J. M. (2018). Optical properties of dissolved organic matter and their relation to mercury concentrations in water and biota across a remote freshwater drainage basin. *Environmental Science & Technology, 52*(6), 3344-3353. https://doi.org/10.1021/acs.est.7b05348

Lescord, G. L., Johnston, T., Branfireun, B. A., & Gunn, J. M. (2019). Mercury bioaccumulation in relation to changing physicochemical and ecological factors across a large and undisturbed boreal watershed. *Canadian Journal of Fisheries and Aquatic Sciences, 76*(12), 2165-2175. https://doi.org/10.1139/cjfas-2018-0465

Lewis, M. E., & Brigham, M. E. (2004). Chapter A5. Section 6.4. B. Low-Level Mercury. *USGS Numbered Series, Techniques of Water-Resources Investigations*(09-A5.6.4.B). https://doi.org/10.3133/twri09A5.6.4.B

Lindqvist, O., Johansson, K., Bringmark, L., Timm, B., Aastrup, M., Andersson, A., et al. (1991). Mercury in the Swedish environment—recent research on causes, consequences and corrective methods. *Water, Air, and Soil Pollution, 55*(1-2), xi-261. https://doi.org/10.1007/BF00542429

Lockhart, W. L., Stern, G. A., Wagemann, R., Hunt, R. V., Metner, D. A., DeLaronde, J., et al. (2005). Concentrations of mercury in tissues of beluga whales (Delphinapterus leucas) from several communities in the Canadian Arctic from 1981 to 2002. *Science of the Total Environment, 351-352*, 391-412. https://10.1016/j.scitotenv.2005.01.050

Lung, J. Y. L. Y., Tank, S. E., Spence, C., Yang, D., Bonsal, B., McClelland, J. W., & Holmes, R. M. (2018). Seasonal and geographic variation in dissolved carbon biogeochemistry of rivers draining to the Canadian Arctic Ocean and Hudson Bay. *Journal of Geophysical Research: Biogeosciences, 123*(10), 3371-3386. https://doi.org/10.1029/2018JG004659

Mason, R. P., Choi, A. L., Fitzgerald, W. F., Hammerschmidt, C. R., Lamborg, C. H., Soerensen, A. L., & Sunderland, E. M. (2012). Mercury biogeochemical cycling in the ocean and policy implications. *Environmental Research, 119*, 101-117. http://doi.org/10.1016/j.envres.2012.03.013

Meili, M. (1991). The coupling of mercury and organic matter in the biogeochemical cycle—towards a mechanistic model for the boreal forest zone. *Water Air & Soil Pollution, 56*(1), 333-347. https://doi.org/10.1007/BF00342281

Messier, D., Ingram, R. G., & Roy, D. (1986). Chapter 20 physical and biological modifications in response to La Grande hydroelectric complex. *44*, 403-424. https://doi.org/10.1016/S0422-9894(08)70913-9

Mierle, G., & Ingram, R. (1991). The role of humic susbstances in the mobilization of mercury from watersheds. *Water Air & Soil Pollution, 56*, 349-357. https://doi.org/10.1007/BF00342282

Mucci, A., Montgomery, S., Lucotte, M., Plourde, Y., Pichet, P., & Tra, H. V. (1995). Mercury remobilization from flooded soils in a hydroelectric reservoir of northern Quebec, La Grande-2: Results of a soil resuspension experiment. *Canadian Journal of Fisheries and Aquatic Sciences, 52*(11), 2507-2517. https://doi.org/10.1139/f95-841

Muir, D., Wang, X., Yang, F., Nguyen, N., Jackson, T., Evans, M., et al. (2009). Spatial trends and historical deposition of mercury in eastern and northern Canada

inferred from lake sediment cores. *Environmental Science & Technology, 43*(13), 4802-4809. https://doi.org/10.1021/es8035412

Nagorski, S. A., Engstrom, D. R., Hudson, J. P., Krabbenhoft, D. P., Hood, E., DeWild, J. F., & Aiken, G. R. (2014). Spatial distribution of mercury in southeastern Alaskan streams influenced by glaciers, wetlands, and salmon. *Environmental Pollution, 184*, 62-72. https://doi.org/10.1016/j.envpol.2013.07.040

Natural Ressources Canada. (1995). *The National Atlas of Canada 5th Edition : Canada Permafrost*. Retrieved from https://open.canada.ca/data/en/dataset/d1e2048b-ccff-5852-aaa5-b861bd55c367.

Natural Ressources Canada. (2019). Download directory and documentation: Elevation data. Retrieved from https://www.nrcan.gc.ca/science-and-data/science-and-research/earth-sciences/geography/topographic-information/download-directory-documentation/17215?_ga=2.81411671.113991294.1568981137-790747878.1568981137

Obrist, D., Kirk, J. L., Zhang, L., Sunderland, E. M., Jiskra, M., & Selin, N. E. (2018). A review of global environmental mercury processes in response to human and natural perturbations: Changes of emissions, climate, and land use. *Ambio, 47*(2), 116-140. http://doi.org/10.1007/s13280-017-1004-9

Obrist, D., Pearson, C., Webster, J., Kane, T., Lin, C.-J., Aiken, G. R., & Alpers, C. N. (2016). A synthesis of terrestrial mercury in the western United States: Spatial distribution defined by land cover and plant productivity. *Science of the Total Environment, 568*, 522-535. https://doi.org/10.1016/j.scitotenv.2015.11.104

Porvari, P., & Verta, M. (2003). Total and methyl mercury concentrations and fluxes from small boreal forest catchments in Finland. *Environmental Pollution, 123*(2), 181-191. https://doi.org/10.1016/S0269-7491(02)00404-9

R Core Team. (2019). R: A language and environment for statistical computing. R Foundation for Statistical Computing.

Ravichandran, M. (2004). Interactions between mercury and dissolved organic matter - A review. *Chemosphere, 55*(3), 319-331. https://10.1016/j.chemosphere.2003.11.011

Richardson, M., Chételat, J., MacMillan, G. A., & Amyot, M. (2020). Mercury concentrations and associations with dissolved organic matter are modified by water residence time in eastern Canadian lakes along a 30° latitudinal gradient. *Limnology and Oceanography*. https://doi.org/10.1002/lno.11580

Riscassi, A. L., & Scanlon, T. M. (2011). Controls on stream water dissolved mercury in three mid-Appalachian forested headwater catchments. *Water Resources Research, 47*, 16. https://10.1029/2011WR010977

Schelker, J., Burns, D. A., Weiler, M., & Laudon, H. (2011). Hydrological mobilization of mercury and dissolved organic carbon in a snow-dominated, forested watershed: Conceptualization and modeling. *Journal of Geophysical Research, 116*(G1). https://doi.org/10.1029/2010JG001330

Schuster, P. F., Schaefer, K. M., Aiken, G. R., Antweiler, R. C., Dewild, J. F., Gryziec, J. D., et al. (2018). Permafrost stores a globally significant amount of mercury. *Geophysical Research Letters, 45*(3), 1463-1471. https://doi.org/10.1002/2017GL075571

Schuster, P. F., Striegl, R. G., Aiken, G. R., Krabbenhoft, D. P., Dewild, J. F., Butler, K., et al. (2011). Mercury export from the Yukon River Basin and potential response to a changing climate. *Environmental Science & Technology, 45*(21), 9262-9267. https://doi.org/10.1021/es202068b

Sellers, P., Kelly, C. A., & Rudd, J. W. (2001). Fluxes of methylmercury to the water column of a drainage lake: The relative importance of internal and external sources. *Limnology and Oceanography, 46*(3), 623-631. https://doi.org/10.4319/lo.2001.46.3.0623

Selvendiran, P., Driscoll, C. T., Bushey, J. T., & Montesdeoca, M. R. (2008a). Wetland influence on mercury fate and transport in a temperate forested watershed. *Environmental Pollution, 154*(1), 46-55. https://doi.org/10.1016/j.envpol.2007.12.005

Selvendiran, P., Driscoll, C. T., & Montesdeoca, M. (2009). Mercury dynamics and transport in two Adirondack lakes. *Limnology and Oceanography, 54*(2), 413-427. https://doi.org/10.4319/lo.2009.54.2.0413

Selvendiran, P., Driscoll, C. T., Montesdeoca, M. R., & Bushey, J. T. (2008b). Inputs, storage, and transport of total and methyl mercury in two temperate forest wetlands. *Journal of Geophysical Research: Biogeosciences, 113*(G2), n/a-n/a. http://doi.org/10.1029/2008jg000739

Shanley, J. B., C., K. N., A., C. T., & Chalmers, A. (2005). Physical controls on total and methylmercury concentrations in streams and lakes of the northeastern USA. *Ecotoxicology, 14*, 125-134. https://doi.org/10.1007/s10646-004-6264-z

Shanley, J. B., Mast, M. A., Campbell, D. H., Aiken, G. R., Krabbenhoft, D. P., Hunt, R. J., et al. (2008). Comparison of total mercury and methylmercury cycling at five sites using the small watershed approach. *Environmental Pollution, 154*(1), 143-154. https://doi.org/10.1016/j.envpol.2007.12.031

Soerensen, A. L., Jacob, D. J., Schartup, A. T., Fisher, J. A., Lehnherr, I., St. Louis, V. L., et al. (2016). A mass budget for mercury and methylmercury in the Arctic Ocean. *Global Biogeochemical Cycles, 30*(4), 560-575. https://doi.org/10.1002/2015GB005280

St. Louis, V. L., Rudd, J. W., Kelly, C. A., Beaty, K. G., Flett, R. J., & Roulet, N. T. (1996). Production and loss of methylmercury and loss of total mercury from boreal forest catchments containing different types of wetlands. *Environmental Science & Technology, 30*, 2719-2729. https://doi.org/10.1021/es950856h

St. Pierre, K. A., Zolkos, S., Shakil, S., Tank, S. E., St. Louis, V. L., & Kokelj, S. V. (2018). Unprecedented increases in total and methyl mercury concentrations downstream of retrogressive thaw slumps in the western canadian Arctic.

Environmental Science & Technology, 52(24), 14099-14109. https://10.1021/acs.est.8b05348

Stoken, O. M., Riscassi, A. L., & Scanlon, T. M. (2016). Association of dissolved mercury with dissolved organic carbon in US rivers and streams: The role of watershed soil organic carbon. *Water Resources Research, 52*(4), 3040-3051. http://doi.org/10.1002/2015wr017849

Stow, J., Krummel, E., Leech, T., & Donaldson, S. (2011). What is the impact of mercury contamination on human health in the Arctic. *AMAP assessment 2011: mercury in the Arctic*, 159-170. https://www.amap.no/documents/download/173/inline

Sunderland, E. M., Gobas, F. A. P. C., Heyes, A., Branfireun, B. A., Bayer, A. K., Cranston, R. E., & Parsons, M. B. (2004). Speciation and bioavailability of mercury in well-mixed estuarine sediments. *Marine Chemistry, 90*(1-4), 91-105. https://10.1016/j.marchem.2004.02.021

Sunderland, E. M., & Mason, R. P. (2007). Human impacts on open ocean mercury concentrations. *Global Biogeochemical Cycles, 21*(4). http://doi.org/10.1029/2006gb002876

Takizawa, Y. (1979). Minamata disease in Japan. *Environmental toxicology and human health, 1*, 325-366.

Tjerngren, I., Karlsson, T., Björn, E., & Skyllberg, U. (2012). Potential Hg methylation and MeHg demethylation rates related to the nutrient status of different boreal wetlands. *Biogeochemistry, 108*(1-3), 335-350. https://doi.org/10.1007/s10533-011-9603-1

Tranvik, L. J., Downing, J. A., Cotner, J. B., Loiselle, S. A., Striegl, R. G., Ballatore, T. J., et al. (2009). Lakes and reservoirs as regulators of carbon cycling and climate. *Limnology and Oceanography, 54*(6part2), 2298-2314. https://doi.org/10.4319/lo.2009.54.6_part_2.2298

Turner, K. W., Edwards, T. W., & Wolfe, B. B. (2014). Characterising runoff generation processes in a lake‐rich thermokarst landscape (Old Crow Flats, Yukon, Canada) using δ18O, δ2H and d‐excess measurements. *Permafrost and Periglacial Processes, 25*(1), 53-59. https://doi.org/10.1002/ppp.1802

U.S. Environmental Protection Agency. (2001). *Method 1630: Methyl mercury in water by distillation, aqueous ethylation, purge and trap, and cold-vapor atomic fluorescence spectrometry*.

U.S. Environmental Protection Agency. (2002). *Method 1631: Mercury in water by oxidation, purge and trap, and cold vapor atomic fluorescence spectrometry*.

Ullrich, S. M., Tanton, T. W., & Abdrashitova, S. A. (2001). Mercury in the aquatic environment: A review of factors affecting methylation. *Critical Reviews in Environmental Science and Technology, 31*(3), 241-293. https://10.1080/20016491089226

UN Environment. (2019). Global mercury assessment 2018. UN environment programme chemicals and health branch Geneva, Switzerland.

UN Environment. (2021). Minamata Convention on Mercury. Retrieved from https://www.mercuryconvention.org/

Vachon, D., Lapierre, J. F., & del Giorgio, P. A. (2016). Seasonality of photochemical dissolved organic carbon mineralization and its relative contribution to pelagic CO2 production in northern lakes. *Journal of Geophysical Research: Biogeosciences, 121*(3), 864-878. https://doi.org/10.1002/2015JG003244

Varty, S., Lehnherr, I., St. Pierre, K., Kirk, J., & Wisniewski, V. (2020). Methylmercury transport and fate shows strong seasonal and spatial variability along a high Arctic freshwater hydrologic continuum. *Environmental Science & Technology*. https://doi.org/10.1021/acs.est.0c05051

Verdon, R., Brouard, D., Demers, C., Lalumiere, R., Laperle, M., & Schetagne, R. (1991). Mercury evolution (1978–1988) in fishes of the La Grande hydroelectric complex, Quebec, Canada. *Water Air & Soil Pollution, 56*(1), 405-417. https://doi.org/10.1007/BF00342287

Vermilyea, A. W., Nagorski, S. A., Lamborg, C. H., Hood, E. W., Scott, D., & Swarr, G. J. (2017). Continuous proxy measurements reveal large mercury fluxes from glacial and forested watersheds in Alaska. *Science of the Total Environment, 599-600*, 145-155. http://doi.org/10.1016/j.scitotenv.2017.03.297

Vidon, P., Carleton, W., & Mitchell, M. J. (2014). Mercury proxies and mercury dynamics in a forested watershed of the US Northeast. *Environmental Monitoring and Assessment, 186*(11), 7475-7488. Article. http://doi.org/10.1007/s10661-014-3941-0

Wang, Q., Kim, D., Dionysiou, D. D., Sorial, G. A., & Timberlake, D. (2004). Sources and remediation for mercury contamination in aquatic systems—a literature review. *Environmental Pollution, 131*(2), 323-336. https://doi.org/10.1016/j.envpol.2004.01.010

Weyhenmeyer, G. A., Fröberg, M., Karltun, E., Khalili, M., Kothawala, D., Temnerud, J., & Tranvik, L. J. (2012). Selective decay of terrestrial organic carbon during transport from land to sea. *Global Change Biology, 18*(1), 349-355. http://doi.org/10.1111/j.1365-2486.2011.02544.x

Zhang, Y., Jacob, D. J., Dutkiewicz, S., Amos, H. M., Long, M. S., & Sunderland, E. M. (2015). Biogeochemical drivers of the fate of riverine mercury discharged to the global and Arctic oceans. *Global Biogeochemical Cycles, 29*(6), 854-864. https://doi.org/10.1002/2015GB005124

Zolkos, S., Krabbenhoft, D. P., Suslova, A., Tank, S. E., McClelland, J. W., Spencer, R. G. M., et al. (2020). Mercury export from Arctic great rivers. *Environmental Science & Technology, 54*(7), 4140-4148. https://doi.org/10.1021/acs.est.9b07145

ANNEXE I

SUPPLEMENTARY INFORMATIONS OF CHAPTER I

This supporting information contains figures of results. The relationship between mercury (Hg) and methylmercury (MeHg) (Figure S1) and the relationships between dissolved and total forms for Hg and MeHg (Figure S2) are provided. These figures guided the methods for final results. A mixed models summary table of the relationship between landscape features and Hg or MeHg concentrations (Table S1) and a summary table of the Chi-square tests on the distributions of Δ Hg and Δ MeHg relative to Δ landscape features (Table S2) are also provided. Both table accompany their respective figure in the main article. Data was collected during summer and fall of 2018, and winter, spring and summer of 2019.

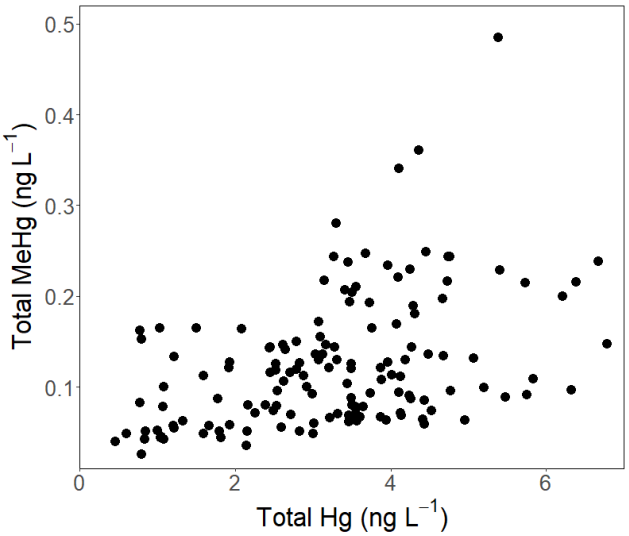

Figure S1. Hg relationship with MeHg (total forms, i.e. unfiltered). Each data point is the average of replicates.

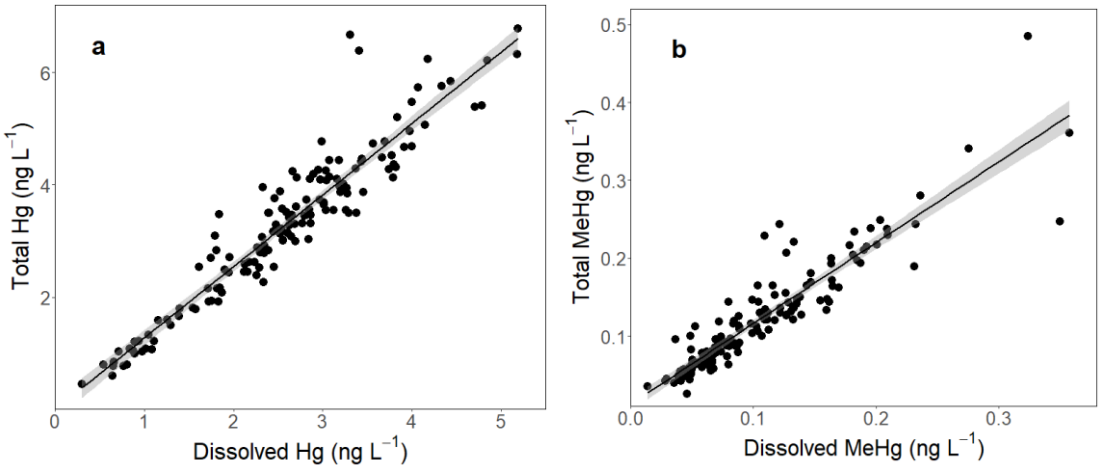

Figure S2. Relationship between dissolved and total forms of Hg (a) and MeHg (b). Grey areas represent error around the curve. Each data point is the average of replicates.

Table S1. Mixed models summary of the relationships between landscape features and Hg or MeHg concentrations

	log(MeHgtot)			**log(Hgtot)**		
Predictors (%)	*Estimates*	*Marginal/Conditional R^2*	Significancy of the model	*Estimates*	*Marginal/Conditional R^2*	Significancy of the model
Total Wetland	0.078	0.19 / NA	***			
All Wetlands * Seasons [Fall]	0.012					
All Wetlands * Seasons [Spring]	0.0020*	0.23 / 0.68	**			
All Wetlands * Seasons [Summer]	0.0065					
All Wetlands * Seasons [Winter]	0.0039					
Water	-0.031	0.60 / NA	***	-0.021	0.61 / NA	***
Water*Seasons [Fall]	-0.038			-0.021		
Water * Seasons [Spring]	-0.012 ***	0.61 / 0.78	***	-0.016	0.74 / NA	***
Water * Seasons [Summer]	-0.031			-0.024		
Water * Seasons [Winter]	-0.023 *			-0.022		
Forest	-0.0065	0.10 / 0.59	***	0.0012	0.013 / NA	
Forest * Seasons [Fall]	-0.043			0.00052		
Forest * Seasons [Spring]	-0.0026	0.18 / 0.72		-0.00083	0.078 / 0.81	
Forest * Seasons [Summer]	-0.0065			0.0023		
Forest * Seasons [Winter]	0.0043			0.0057		

** $p<0.05$ ** $p<0.01$ *** $p<0.001$*

Table S2. Summary of Chi-square tests on distributions of Δ Hg and Δ MeHg concentrations relative to Δ landscape features

Landscape variable	Mercury species	$\chi 2$
% Water	Hg	25.024 ***
% Water	MeHg	32.136 ***
% All Wetlands	MeHg	43.099 ***
% Forest	Hg	4.5366
% Forest	MeHg	5.0741

** $p<0.05$ ** $p<0.01$ *** $p<0.001$*

ANNEXE II

SUPPLEMENTARY INFORMATIONS OF CHAPTER II

This supporting information includes a figure of daily mean air temperature during sampling periods, in order to show the seasonality across our study area (Figure S3). It also provides a figure of Tukey HDS post-hoc tests results showing differences in seasonal slopes of the relationships involving Hg, MeHg and DOC (Figure S4) and a summary table of the linear relationships involving Δ Hg:DOC ratios, Δ MeHg:DOC ratios and Δ cDOM:DOC ratios in relation to Δ d-excess (Table S3). Both figure S4 and table S3 accompany their respectives figures in the main article (Chapter 2). Data were collected during summer and fall of 2018, and winter, spring and summer of 2019.

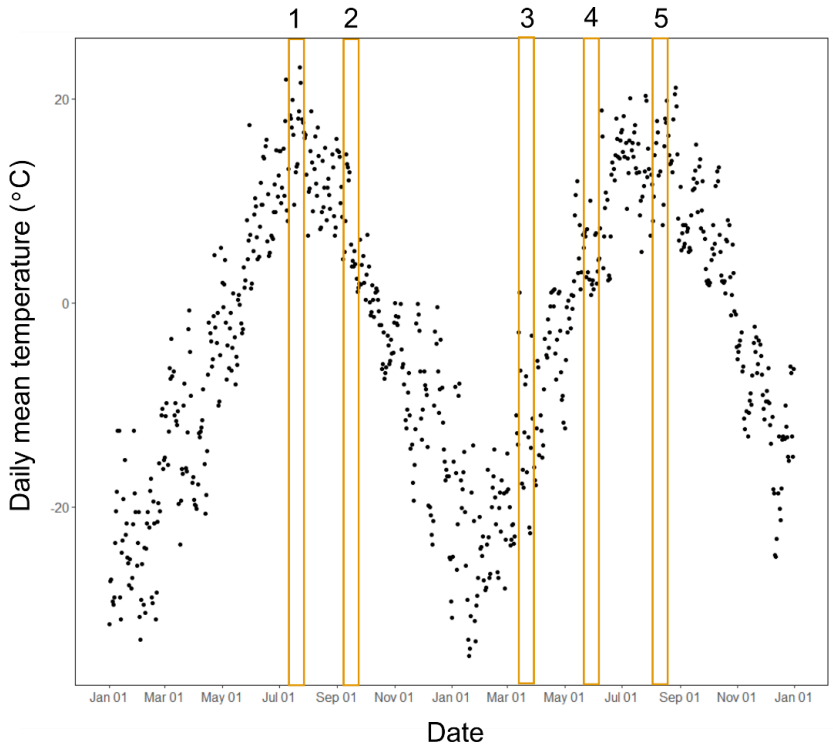

Figure S3. Daily mean air temperature from January 1st 2018 to January 1st 2020 in relation to sampling campaigns of summer 2018 (1), fall 2018 (2), winter 2019 (3), spring 2019 (4) and summer 2019 (5). Data retrieved from historical climatic data from government of Canada (Government of Canada, 2020a).

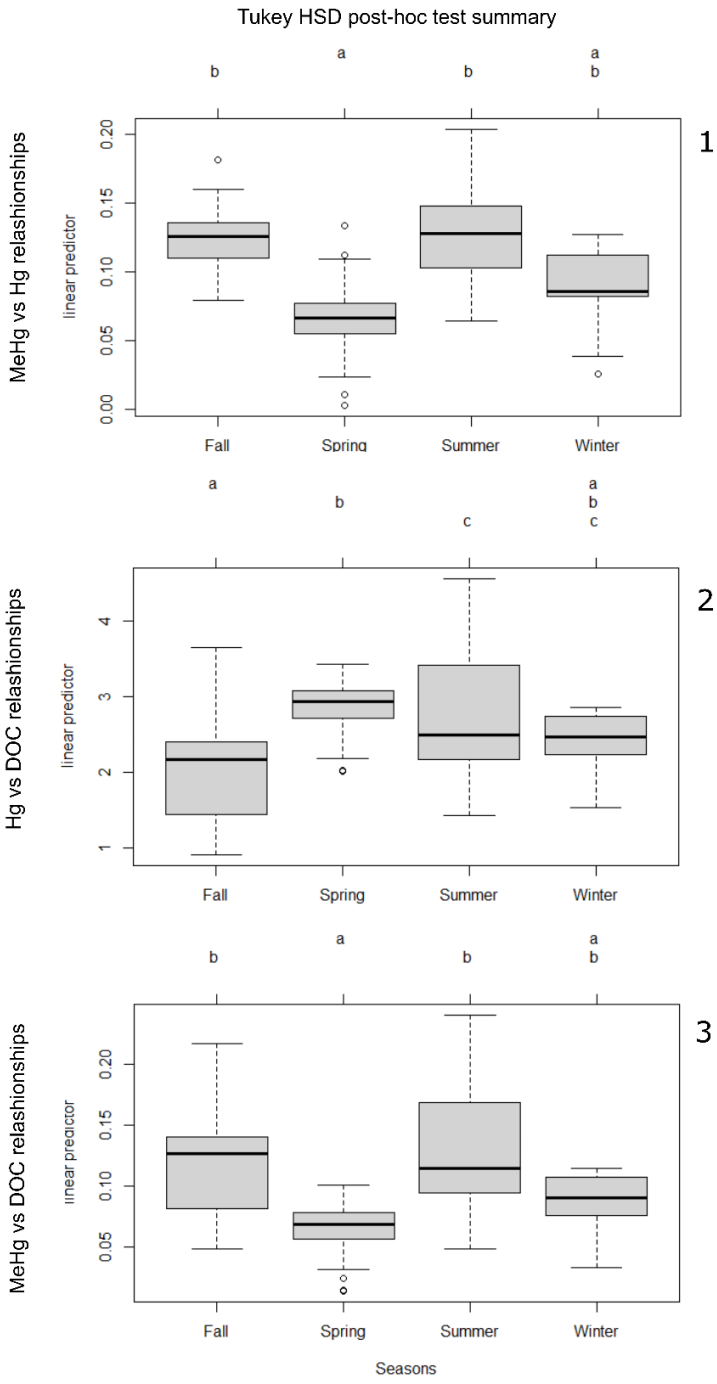

Figure S4. Outcome of Tukey post-hoc tests showing differences in seasonnal slopes of the relationships between 1) MeHg and Hg, 2) Hg and DOC and 3) MeHg and DOC.

Table S3. Summary of linear regressions involving Δ Hg:DOC ratios, Δ MeHg:DOC ratios, Δ cDOM:DOC ratios in relation to Δ d-excess.

	Hg:DOC vs d-excess	**MeHg:DOC vs d-excess**	**cDOM:DOC vs d-excess**
Predictors	*Estimates*	*Estimates*	*Estimates*
(Intercept)	0.00014	-0.00110 **	0.00812
dexcess	0.00997 ***	-0.00021 **	0.01068 ***
Observations	207	207	207
R^2 / R^2 adjusted	0.246 / 0.242	0.042 / 0.038	0.168 / 0.164

** p<0.05 ** p<0.01 *** p<0.001*